NASA TECHNICAL NOTE



NASA TN D-7182

NASA TN D-7182



# DESCRIPTION AND CALIBRATION OF THE LANGLEY 6- BY 19-INCH TRANSONIC TUNNEL

*by Charles L. Ladson*

*Langley Research Center*
*Hampton, Va. 23365*

NATIONAL AERONAUTICS AND SPACE ADMINISTRATION • WASHINGTON, D. C. • MAY 1973

| 1. Report No. NASA TN D-7182 | 2. Government Accession No. | 3. Recipient's Catalog No. |
|---|---|---|
| 4. Title and Subtitle<br>DESCRIPTION AND CALIBRATION OF THE LANGLEY 6- BY 19-INCH TRANSONIC TUNNEL | | 5. Report Date<br>May 1973<br>6. Performing Organization Code |
| 7. Author(s)<br>Charles L. Ladson | | 8. Performing Organization Report No.<br>L-8680<br>10. Work Unit No.<br>501-06-05-02 |
| 9. Performing Organization Name and Address<br>NASA Langley Research Center<br>Hampton, Va. 23665 | | 11. Contract or Grant No.<br>13. Type of Report and Period Covered<br>Technical Note |
| 12. Sponsoring Agency Name and Address<br>National Aeronautics and Space Administration<br>Washington, D.C. 20546 | | 14. Sponsoring Agency Code |

15. Supplementary Notes

16. Abstract

This report presents a description and calibration of the Langley 6- by 19-inch transonic tunnel which is a two-dimensional facility with top and bottom slotted walls used for testing two-dimensional airfoil sections. Basic tunnel-empty Mach number distributions and schlieren flow photographs as well as integrated normal-force coefficients, pitching-moment coefficients, surface-pressure distributions, and schlieren flow photographs of an NACA 0012 airfoil calibration model are presented. The Mach number capability of the facility is from 0.5 to about 1.1 with a corresponding Reynolds number range of $1.5 \times 10^6$ to $3.0 \times 10^6$ based on a 10.2-cm (4.0-in.) model chord. Comparisons of experimental results from the tests with previous data are also presented.

| 17. Key Words (Suggested by Author(s))<br>Transonic tunnels<br>Two-dimensional tunnels<br>Airfoils | 18. Distribution Statement<br>Unclassified – Unlimited | | |
|---|---|---|---|
| 19. Security Classif. (of this report)<br>Unclassified | 20. Security Classif. (of this page)<br>Unclassified | 21. No. of Pages<br>62 | 22. Price*<br>$3.00 |

*For sale by the National Technical Information Service, Springfield, Virginia 22151

# DESCRIPTION AND CALIBRATION OF THE LANGLEY 6- BY 19-INCH TRANSONIC TUNNEL

By Charles L. Ladson
Langley Research Center

## SUMMARY

The Langley 6- by 19-inch transonic tunnel was placed in operation in early 1971. This facility is a two-dimensional tunnel with top and bottom slotted walls which operates on direct blowdown from a supply of dry compressed air. The tunnel is capable of operation at Mach numbers from 0.5 to 1.1 with a corresponding Reynolds number range of about $1.5 \times 10^6$ to $3.0 \times 10^6$ based on a 10.2-cm (4.0-in.) model chord. Tunnel-empty calibrations show the local Mach number distribution obtained from wall static pressures varies less than ±0.005 from the average value in the test region occupied by the model at all Mach numbers. As part of the tunnel calibration, typical surface oil flow photographs, schlieren flow photographs, surface-pressure distributions, and integrated normal-force and pitching-moment coefficients have been obtained on an NACA 0012 airfoil section. The integrated pressure data obtained on the model have been compared with results from two other small transonic facilities and the results show that the 6- by 19-inch transonic tunnel produces slightly higher normal-force coefficients and a negative increment in pitching moment. The pressure data show this results from the farther rearward location of the shock wave on the upper surface for the same Mach number and angle of attack. The data were also compared with results from two closed-throat tunnels at Mach numbers up to 0.80 and show good agreement at low angles of attack up to $M = 0.70$ when the data from the slotted tunnel have been corrected for lift-interference effects. As would be expected, the theoretical corrections do not give good results when large areas of supercritical flow exist on the model. When lift-interference effects are included, good agreement between the data and two theoretical subcritical pressure distributions is also shown.

## INTRODUCTION

Two-dimensional airfoil data at subsonic and transonic speeds are vitally needed in the design of wing sections for military and civilian aircraft as well as propeller and rotor sections for V/STOL aircraft. By use of surface-pressure distributions, force and moment coefficients, and flow photographs the effects of variables such as thickness,

thickness distribution, leading-edge radius, and camber may be studied independently. With the current interest in advanced transports and V/STOL configurations, the needs for this type of information from low subsonic to sonic speeds are evident. From the late 1950's to 1970 the only two-dimensional airfoil research conducted at Langley Research Center was the recent work on the supercritical wing section (refs. 1 to 4) in the Langley 8-foot transonic pressure tunnel. During this time period the small two-dimensional transonic tunnels which existed were dismantled or destroyed.

To provide the capability for testing small two-dimensional models at transonic speeds, a design was begun in late 1968 to modify the existing 22-inch transonic tunnel (a three-dimensional facility) to a 6- by 19-inch two-dimensional tunnel using as much of the existing hardware as possible. This modification was completed in 1970 and routine testing in the facility began early in 1971. This facility, designated as the Langley 6- by 19-inch transonic tunnel, is a two-dimensional, slotted-wall, vertical wind tunnel operating on direct blowdown from a tank farm of dry, compressed air. In its present configuration, this wind tunnel is capable of operation at Mach numbers from 0.5 to about 1.1. For this Mach number range the Reynolds number based on a 10.2-cm (4.0-in.) model chord varies from about $1.5 \times 10^6$ to $3.0 \times 10^6$.

The purpose of this paper is to present a description and calibration of the facility including its history. Test results, obtained for the NACA 0012 airfoil section at angles of attack up to $10^\circ$, are presented in the form of typical surface oil flow photographs, schlieren flow photographs, integrated normal-force and pitching-moment coefficients, and local surface-pressure distributions. The data for the NACA 0012 section are compared with results from other transonic facilities. Some effects of slotted-wall open-area ratio and wake survey rake (blockage) are also discussed.

## SYMBOLS

Values are given in both SI and U.S. Customary Units. The measurements and calculations were made in U.S. Customary Units.

$c$ airfoil chord, 10.2 cm (4.0 in.)

$c_l$ section lift coefficient

$c_m$ section moment coefficient about quarter chord,

$$\int_0^1 C_{p_{lower}}\left(0.250 - \frac{x}{c}\right)d\left(\frac{x}{c}\right) - \int_0^1 C_{p_{upper}}\left(0.250 - \frac{x}{c}\right)d\left(\frac{x}{c}\right)$$

$c_n$ section normal-force coefficient, $\int_0^1 C_{p_{lower}} d\left(\frac{x}{c}\right) - \int_0^1 C_{p_{upper}} d\left(\frac{x}{c}\right)$

$C_p$ pressure coefficient, $\frac{p_l - p}{q}$

d slot width (see fig. 4(c)), cm (in.)

M average test-section Mach number (average of $M_l$ from station -5.1 cm to 5.1 cm (-2.0 in. to 2.0 in.))

$M_l$ local Mach number

$M_{TC}$ test-chamber Mach number

p stream static pressure (computed from M and $p_t$)

$p_l$ local static pressure

$p_t$ stream stagnation pressure, $kN/m^2$ ($lb/in^2$)

q stream dynamic pressure (computed from M and p), $kN/m^2$ ($lb/in^2$)

R Reynolds number based on model chord

$T_t$ stagnation temperature, K ($^oR$)

x,y longitudinal and vertical distances on airfoil and tunnel axes (origin at leading edge of chord line for airfoil or at center of window for tunnel), cm (in.)

$\alpha$ angle of attack, deg

$\alpha_c$ angle of attack corrected for lift interference, deg

$\sigma$ open area ratio of slotted walls

## APPARATUS

### History of Facility

The Langley 6- by 19-inch transonic tunnel (fig. 1) is a modification of the Langley 24-inch high-speed tunnel (fig. 2) which was designed in 1933 and became operational

in 1934. Because the 24-inch high-speed tunnel operated on the induction principle with atmospheric air as the test medium, an enclosure, shown in figure 3, was added in 1949 to recycle the air from the induction jet thus reducing humidity effects. To make the enclosure as small as possible (and increase the performance capability of the tunnel) the length of the diffuser was decreased by about 3.66 m (12 ft) at the same time (compare figs. 2 and 3). In 1952, the circular closed-throat test section was converted to a slotted octagonal section which measured 50.8 cm (20 in.) across the flats and called the 22-inch transonic tunnel. A settling chamber and hydraulically operated, manually controlled air regulating valve were also added at this time to permit direct blowdown operation on dry compressed air. In 1970 the octagonal test section was removed and the 6- by 19-inch transonic test section installed. Thus, the present facility uses a settling chamber, diffuser, test chamber, and air-control system from previous tunnels and is by no means an optimum design tunnel.

## General Description

The Langley 6- by 19-inch transonic tunnel is a two-dimensional facility with solid parallel sidewalls and top and bottom slotted walls and operates on direct blowdown from a supply of dry compressed air. Photographs and drawings of the facility are presented in figures 1 and 4. The settling-chamber stagnation pressure is regulated by a manually controlled, hydraulically operated plug valve. The Mach number is controlled from about 0.5 to 1.15 by varying the stagnation pressure; hence, there is no independent control of Reynolds number for this facility.

Air enters the 1.63-m-diameter (64-in.) circular cross-section settling chamber radially through a manifold with 16 openings (fig. 4(a)), passes through a baffle plate of about 50 percent porosity and four fine mesh screens to reduce turbulence, and then enters a transition section to the 15.2-cm (6-in.) by 48.3-cm (19-in.) rectangular test section. The contraction ratio between the circular settling chamber and the rectangular test section is about 28:1.

Details of the test section are shown in figure 4(b). The rectangular portion begins at station -127.3 cm (-50.1 in.) and ends at 51.1 cm (20.1 in.). Circular windows with a diameter of 22.9 cm (9 in.) are located in the sidewalls and provide for the model support. The center of the windows are at tunnel station 0. The details of the top and bottom slotted walls are shown in figure 4(c). Four longitudinal slots are located in both of the 15.2-cm-wide (6-in.) walls and consist of three full slots and a half slot on each side of the wall (figs. 1(b) and 4(c)). The slots begin at station -58.4 cm (-23 in.), have a linear divergence to station -27.9 cm (-11.0 in.), and a constant width to station 8.5 cm (3.33 in.). From this point, the slots again diverge linearly to a fully open condition at station 38.1 cm (15.0 in.). Three interchangeable sets of slots were constructed having

open area ratios of 0.040, 0.125, and 0.250. The top and bottom slotted walls are adjustable so that their slope with respect to the tunnel axis may be changed. For these tests they were set parallel to the tunnel axis, as were the fixed solid sidewalls.

Air which has passed through the slotted walls into the test chamber is returned to the airstream over reentrant flow fairings which begin at tunnel station 33.3 cm (13.1 in.). The minimum cross-section area in this mixing region is located at station 51.1 cm (20.1 in.) and is 20 percent larger than the test-section area to provide space for the low energy reentrant flow to return to the main airstream. From this point, the air enters abruptly into the existing conical diffuser of the 24-inch high-speed tunnel which exhausts to atmosphere. Because of the sudden large increase in area, the diffuser is very inefficient and the test-chamber static pressure remains near atmospheric pressure throughout the Mach number range. Because the diffuser is inefficient, the rate of change of Mach number with stagnation pressure is low and, for this tunnel, the control of Mach number is enhanced. Typical plots of Reynolds number, stagnation pressure and temperature, and dynamic pressure for the tunnel empty with an open area ratio of 0.125 are presented in figure 5 as a function of Mach number.

## MODELS

A typical model photograph is presented in figure 6. Two models are constructed for each airfoil shape: a solid model for schlieren flow photography and an instrumented model for surface-pressure distributions. The solid model is mounted in glass windows by means of dowel pins so that an unobstructed view of the flow field is obtained. The instrumented models are mounted in plexiglass windows. In general, 22 orifices are located on each surface in chordwise rows 12.5-percent span on either side of the midspan. Slots are milled in the airfoil surface and tubes are placed in the slot and covered over with epoxy. The orifices are then drilled from the opposite side of the model so there are no surface irregularities near the orifice row. Typically, the orifices have a diameter of 0.0343 cm (0.0135 in.) (number 80 drill) and are located at 1.25-, 2.5-, 5.0-, 7.5-, 10-, 15-, 20-, 25-, 30-, 35-, 40-, 45-, 50-, 55-, 60-, 65-, 70-, 75-, 80-, 85-, 90-, and 95-percent-chord stations. Models have been constructed of both brass and stainless steel but the steel models are preferred since better machining accuracy can be obtained and the surface is not as easily damaged as the brass. Construction accuracies of $2 \times 10^{-4}$ chord or better are desirable for models of this size.

Ordinates for the NACA 0012 airfoil section were obtained from the equations in reference 5 and are presented in table I. Also shown in the table are the ordinates measured on the brass model after construction. The model had a 10.2-cm (4.0-in.) chord and completely spanned the 15.2-cm (6-in.) width of the tunnel.

## TESTS AND PROCEDURES

### Test Procedure

All data were obtained by varying the stagnation pressure until the desired test-chamber Mach number was obtained. While the Mach number was held constant, the data were recorded and then the pressure varied until the next desired Mach number was obtained. The Mach number is displayed on the control console by use of an aircraft-type Mach meter. The settling-chamber pressure and the static pressure in the tunnel enclosure are used for the Mach indicator and are also recorded. From tunnel-empty calibration curves, the relationship between the average test-section Mach number and the indicated Mach number based on these two pressures can be determined. The Mach number range for this facility can be varied from about 0.5 to 1.15. The drag coefficient of airfoils is measured by means of a wake survey rake, shown in figure 7. About 70 pitot pressure tubes are located on the rake. The survey rake extends about two model chords above and below the model and is located 1.25 chords downstream of the trailing edge. Schlieren flow photographs are usually obtained in separate tests with the model mounted in glass windows so that the entire flow field is visible. The flow-field photographs are recorded on 35-mm motion-picture film and frame rates of about 9, 18, and 36 frames per second are available. A flashing mercury lamp synchronized with the camera and with an exposure time of about 4 microseconds is used as the light source. This system is described in detail in reference 6. Tests are usually made by varying the Mach number from about 1.1 to 0.6 continuously and recording the data on a 30.48-m (100-ft) roll of film. Individual frames or a sequence of frames (as shown in ref. 6) can then be selected to show the desired flow conditions.

### Tunnel Empty

The Mach number distribution of the tunnel was determined from measurements of stagnation pressure and sidewall surface pressures. The stagnation pressure was obtained from a total head probe located in the settling chamber, whereas the surface pressures were obtained from flush sidewall static orifices. The sidewall orifices are located on the longitudinal center line along one side of the tunnel from the transition section, station -112 cm (-44 in.), to the diffuser, station 45.7 cm (18 in.). A vertical row of orifices is located at tunnel station 0. Solid metal plates were installed in the test-section windows and pressure orifices were located in these on both sides of the tunnel for symmetry checks. Tests were conducted at stagnation pressures corresponding to a range of Mach numbers from about 0.5 to 1.15 with the three different open-area-ratio walls and with the rake in place for the 0.125 open-area-ratio walls. Schlieren flow photographs were also obtained for the tunnel-empty condition.

## NACA 0012 Airfoil

For the tests with the NACA 0012 airfoil section installed in the tunnel, model surface pressures, schlieren flow photographs, and surface oil flow photographs were obtained. For the pressure tests, data were recorded at angles of attack from about $0^{\circ}$ to $10^{\circ}$ in $2^{\circ}$ increments over the Mach number range from 0.5 to 1.15. Schlieren flow photographs were obtained only at angles of attack of $0^{\circ}$, $4^{\circ}$, and $8^{\circ}$ over a Mach number range from about 0.7 to 1.1.

## DATA ACQUISITION AND REDUCTION

All orifices, whether on the tunnel wall, model, or survey rake, are connected to electrical strain-gage-type pressure transducers. The output of the transducer is recorded on 2.54-cm (1-in.) 16-track magnetic tape in a digital format. The data acquisition system (fig. 8(a)) was capable of recording only 45 channels of data; thus, a bank of relays was used as a multiplexing device so that a maximum of 135 analog channels could be recorded. The time to record all channels is less than 1 second. The output from the transducers can also be displayed in bar graph form on a cathode ray tube so that a real-time visual display of the trends of the data being recorded is available. (See fig. 8(b).) After a series of tests are completed, the data are processed and reduced to coefficient form. The model surface pressures are integrated as a function of airfoil chord and thickness to provide the section normal-force, pitching-moment, and chord-force coefficients. The data recorded from the pitot pressure probes on the wake survey rake are also integrated to provide the section drag coefficient.

## ACCURACY

All pressures on the tunnel sidewall and model surface were measured by strain-gage-type pressure transducers with a full-scale range of 206 $kN/m^2$ absolute (30 psia). Repeat calibrations of these instruments have shown their output to be linear and repeatable within $\pm 0.25$ percent of full-scale output and the hysteresis to be less than 0.10 percent of full scale. Repeatability of data during a given run is indicated by repeat data points at $M \approx 0.5$ for some of the data presented herein. The geometric angle of attack of the model is accurate to $\pm 0.1^{\circ}$.

## PRESENTATION OF RESULTS

The results of this investigation are presented in the form of basic data plots and flow photographs. The tunnel-empty calibration results are presented first and the

results for the NACA 0012 airfoil section calibration model presented next. An index to the figures follows:



## DISCUSSION

### Tunnel-Empty Calibration

Mach number distributions.- Sidewall static-pressure measurements were made for the tunnel-empty condition to determine the Mach number distribution in both the streamwise and normal-to-stream directions. For all of these tests, the tunnel top and bottom slotted walls were set parallel to the airstream. Results of these tests are presented in figures 9 to 12 as plots of local Mach number against tunnel station. Shown in these figures are the test-chamber Mach number $M_{TC}$ and the average test-section Mach number M. The test-chamber Mach number is computed from the stagnation pressure and the static pressure in the housing around the tunnel. The average test-section Mach number is defined as the longitudinal average of the local Mach numbers measured within 1/2 model chord on either side of station 0. If M had been defined as the average of the local Mach numbers for 1 model chord on either side of station 0, the difference in average Mach numbers between test regions of 1 chord and 2 chords would be $\pm 0.002$ or less. For the open area ratio of 0.040 (see fig. 9) an increase in $M_l$ above M is usually observed downstream of station 7 cm (3 in.) and is much more

pronounced beyond station 10 cm (3.97 in.) at the supersonic speeds. Because this occurs at the longitudinal station at which the slots begin to diverge, it is probably the result of a rapid expansion through the slots and could be eliminated by increasing the length of the constant-width portion of the slot. In contrast, the 0.250-open-area-ratio walls (see fig. 12) show an overexpansion at supersonic speeds which occurs between stations -40 cm (-16 in.) and -7 cm (-3 in.). This is probably caused by too large a divergence angle for the slots and could be alleviated by decreasing the divergence angle and changes in the length of the divergence section. For the 0.125-open-area-ratio walls (see figs. 10 and 11) any local Mach number is generally within ±0.005 of the average Mach number for 1 model chord on either side and above or below tunnel station 0 with no unusual gradients elsewhere. As a result, this slot configuration has been used for all data presented herein unless otherwise noted.

Wake-rake blockage.- A wake survey rake for use in measuring the airfoil drag coefficient was installed for some of the tests. The results of the tunnel calibration with this rake in place are shown in figure 13. The rake was fabricated after the test section had been constructed and the lateral blockage is about 5 percent at tunnel center line with no sidewall relief, although some three-dimensional relief would be expected. The data indicate that over a large portion of the Mach number range tested, the rake caused blockage which produced a Mach number gradient through tunnel station 0. The maximum Mach number reached at the station of the rake leading edge, 18 cm (7 in.), was only 0.9 but the flow accelerates past the rake and indicated local Mach numbers higher than the average stream valve were recorded downstream for some cases. Contouring of the sidewalls might provide some relief of the blockage problem which is due to the reduction in cross-sectional area of the stream in the region of the rake. (The maximum cross section of the rake is about 3.5 percent of the test-section area.) For the present rake geometry, it appears that data can be obtained only at Mach numbers up to about 0.90 if excessive Mach number gradients over the region occupied by the model are to be avoided.

Flow-field disturbances.- Schlieren flow photographs were obtained for the tunnel empty both with and without the rake installed and typical pictures are presented in figure 14. Without the rake (see fig. 14(a)) some slight random and very weak symmetrical disturbances are observed at Mach numbers below 1.0. For the supersonic speeds no disturbances are noted. With the rake installed a series of weak normal-to-stream disturbances are noted from $M \approx 0.9$ to 0.98. At $M = 1.0$ these disturbances form a fairly strong normal shock wave that moves downstream as the Mach number is increased further. The sidewall Mach number distribution (see fig. 13) shows a gradient along the tunnel wall and not a jump as would be expected for a normal shock wave. This is the result of interaction between the shock wave and the tunnel sidewall boundary layer.

## Results From 6- by 19-Inch Transonic Tunnel for NACA 0012 Airfoil

Surface flow distortions.- To examine the two-dimensionality of the flow over the model, surface oil flow photographs were obtained over the NACA 0012 airfoil sections. Rows of small dots of a mixture of lampblack and SAE 30 oil were placed on the model before it was inserted into the tunnel. The tunnel was started and the speed increased to the desired value and held constant for 10 to 20 seconds. After a rapid tunnel shutdown the model was removed and photographed. Since the flow pattern begins to form as soon as the airflow is started, useful results could not be obtained at speeds higher than $M \approx 0.65$.

The results obtained at $M = 0.50$ and $M = 0.65$ are presented in figure 15. At $M = 0.50$ (see fig. 15(a)), the photograph for $\alpha = 8^{\circ}$ shows that the flow is two-dimensional with only a slight inflow noted near the wall. As the angle of attack is increased to $10^{\circ}$, reverse flow is noted along the center line and a weak three-dimensional flow field is beginning to form on either side of the center line. As the angle of attack is increased to $12^{\circ}$, the unsymmetrical three-dimensional flow field is fully formed and reverse flow is observed along the midspan of the airfoil. Similar effects are noted at $M = 0.65$ (see fig. 15(b)) but at lower angles of attack. As shown by data presented later (fig. 23), the angles of attack at which the three-dimensional effects are noted are essentially that for maximum normal-force coefficient. Thus, when maximum normal force is reached and the upper-surface flow separates, three-dimensional flow fields are observed in the separated region. Similar results have been observed in other facilities and some detailed results are presented in reference 7.

It is also noted in figure 15 that there is little inflow indicated on the model surface at the tunnel wall boundary. Thus, from the data presented herein, it cannot be concluded that wall boundary-layer treatment (suction, blowing, etc.) would or would not delay separation or otherwise alter the flow over the airfoil to provide improved two-dimensionality of the flow. Some results of the wall treatment are also presented in reference 7.

Wall boundary interference.- The NACA 0012 airfoil was tested with each of the three different open-area-ratio walls with which the tunnel had been calibrated. The purpose was to determine the effects of open area ratio on the data and to compare the results with the theoretical effects of wall interference. The normal-force and pitching-moment results are presented in figure 16 and selected pressure distributions are presented in figure 17.

References 8 and 9 present the theoretical lift-interference corrections for slotted tunnels as a function of the tunnel and slot geometry, open area ratio, and model chord. These references show that the effective angle of attack is reduced as the open area is

increased; therefore, and for the geometry of the 6- by 19-inch transonic tunnel with a 10.2-cm-chord (4.0-in.) model, the corrected angle of attack is as follows:

$$\alpha_c = \alpha - 2.16c_l \qquad (\sigma = 0.040)$$

$$\alpha_c = \alpha - 2.79c_l \qquad (\sigma = 0.125)$$

$$\alpha_c = \alpha - 2.88c_l \qquad (\sigma = 0.250)$$

Based on these calculations, the data for the two larger open area ratios should be essentially the same, while the data for the smallest ratio should exhibit characteristics of a slightly higher angle of attack with the magnitude of the difference increasing with $c_l$ (or angle of attack). The experimental results (see fig. 16(a)) show that, as the open area ratio is increased from 0.040 to 0.125, the normal-force coefficient decreases as indicated by theory. For Mach numbers of 0.90 and less and angles of attack below $6.5^\circ$, the magnitude of the decrease is about that indicated by theory. At the higher angles of attack and Mach numbers, the magnitudes are much greater than theory would predict. Increasing the open area ratio from 0.125 to 0.250 produces small effects on the normal force at the lower angles of attack and Mach numbers, but the effects are not always in the direction predicted by the theory. The pitching-moment data (see fig. 16(b)) show results similar to those observed for the normal force.

Typical pressure distributions are shown in figure 17 for angles of attack of $4.5^\circ$ and $10.5^\circ$ at Mach numbers of 0.56 and 1.01. No consistent trend is noted at $M = 0.56$ but an increase in surface pressure with decreasing open area ratio is noted at $M = 1.01$. This effect is noted on both surfaces of the airfoil at $\alpha = 4.5^\circ$ (see fig. 17(a)) but is most pronounced on the lower surface at $\alpha = 10.5^\circ$ (see fig. 17(b)).

Although no conclusive determinations of lift interference or corrections to the data can be obtained from this limited investigation, it does show the magnitude of effects which can be expected from changes in open area. With the open area held constant for a series of airfoil tests the results should be valid for determining relative effects, although the absolute magnitude of any particular parameter will be subject to a correction.

Wake-rake blockage.- As mentioned previously, installation of a wake survey rake in the tunnel with the 0.125-open-area-ratio walls produced blockage and resulted in a Mach number gradient around station 0 which was excessive at average stream Mach numbers above about 0.90. The NACA 0012 airfoil was tested with and without the survey rake in place to determine the effect of this rake blockage on the airfoil normal force, pitching moment, and surface-pressure distributions and the results are presented in figures 18 and 19. The results show that there is little or no consistent effect of the rake

on normal force and pitching moment at Mach numbers of about 0.9 and below for angles of attack of $4^{\circ}$ or less and for Mach numbers below about 0.7 at an angle of attack of $6^{\circ}$. Beyond these limits large differences are observed. The pressure distributions in figure 19 show that at low speeds ($M \approx 0.55$) where the integrated forces agree, the local pressures also agree. At the higher speeds ($M \approx 0.90$) the differences noted are a result of a more forward location of the shock wave on the model with the rake in place. This more forward location of the shock is a result of a lower effective Mach number with the rake in place. Thus, the present rake configuration can only be used at Mach numbers below about 0.9 for angles of attack up to about $4^{\circ}$.

Flow-field disturbances.- Schlieren flow photographs for the NACA 0012 airfoil at angles of attack of $0^{\circ}$, $4^{\circ}$, and $8^{\circ}$ are presented in figure 20 for selected Mach numbers between 0.7 and 1.05. These are selected frames from 35-mm motion pictures which were taken at a speed of about 18 frames per second. No discussion of the flow photographs will be made but the pictures are presented to show the flow pattern over the airfoil and indicate the capabilities of the 6- by 19-inch transonic tunnel. The scale and pointer in the photographs indicate the test Mach number.

## Comparison of Results From 6- by 19-Inch Transonic Tunnel With Other Experiments

The integrated pressure data obtained on the NACA 0012 airfoil section in the 6- by 19-inch transonic tunnel are compared with results from the Langley airfoil test apparatus (ATA) and the Langley 4- by 19-inch semiopen tunnel taken from reference 10 and the results are shown in figure 21. Both of these facilities had 4- by 19-inch rectangular test sections, used 10.2-cm-chord (4.0-in.) models, and were blowdown tunnels. The ATA had slotted walls similar to the present 6- by 19-inch tunnel whereas the semiopen tunnel had solid sidewalls but open boundaries on the top and bottom which were enclosed in a chamber with connecting ducts. The data shown from these tunnels are for the same constant stagnation pressure and the Reynolds number varied from about $1.7 \times 10^6$ (based on model chord) at $M = 0.5$ to $2.2 \times 10^6$ at $M = 1.1$. For the 6- by 19-inch tunnel the Reynolds number varies from about $1.5 \times 10^6$ to about $3.0 \times 10^6$ over the same Mach number range.

The normal-force coefficient (see fig. 21(a)) obtained in the 6- by 19-inch transonic tunnel shows good agreement with data from the other facilities at the low Mach numbers but is generally higher as the Mach number is increased, especially at the two highest angles of attack. However, the pitching moment (see fig. 21(b)) shows a negative increment when compared to the data from the other facilities. Typical pressure distributions from the 6- by 19-inch transonic tunnel and the ATA are presented in figure 22. The

data from the ATA are unpublished, but were obtained during the tests reported in reference 10. The results show that the higher normal force and negative pitching-moment increment result from a more rearward shock-wave location on the airfoil in the 6- by 19-inch transonic tunnel. Also, the data for the low angle of attack at the higher test Mach number presented show lower surface pressures near the trailing edge of both surfaces in the 6- by 19-inch transonic tunnel. The reasons for the difference in shock location cannot be positively identified, but are probably the results of difference in model aspect ratio, tunnel geometry, and longitudinal location of boundary-layer transition on the model. The aspect ratio of the model (span/chord) was 1.0 for the ATA and 1.5 for the 6- by 19-inch transonic tunnel. For the higher aspect ratio, the tunnel sidewalls are farther removed from the chordwise orifice row and at the higher angles of attack, where wall effects would be expected to have more effect on the data, the flow over the center portion of the model might be less affected, thus yielding higher normal force (or less separation). The ratio of tunnel to plenum-chamber cross-section area for the two facilities is also quite different. This could lead to a different acoustic environment in the facilities which in turn could affect the location of boundary-layer transition. The transition location would also be subject to effects of differences in tunnel-air-turbulence levels and slight differences in model contour. Since the Reynolds number range of the two facilities is very close, it is not thought to be an influencing factor in the data.

The data comparison shown in figure 21 was from slotted and semiopen test sections and the theoretical corrections to angle of attack for lift interference in all three facilities were essentially the same. In figure 23 the data from the 6- by 19-inch transonic tunnel are compared with results from two closed-throat tunnels at Mach numbers up to 0.80 taken from references 11 and 12. For closed-throat tunnels the correction for angle of attack due to lift interference is essentially zero.

As expected, the uncorrected data from the 6- by 19-inch transonic tunnel have a lower lift-curve slope at the lower Mach numbers but when the data are corrected for the lift interference (see section entitled "Wall boundary interference") the agreement between the slopes is good up to $M = 0.70$. However, this correction is only valid where there is no, or only small amounts of, supercritical flow over the airfoil and the results of figure 23 show the agreement of the data breaks down at decreasing angles of attack as the Mach number is increased. At $M = 0.80$, where the flow photographs show large regions of supercritical flow, the initial lift-curve slope shows agreement but at lifting conditions the uncorrected data show as good or even better agreement than the corrected data. This shows the expected limits of the theoretical interference corrections but still leaves unanswered the corrections for slotted-wall-tunnel data at high lift coefficients and high transonic Mach numbers. It should also be noted that the agreement between

the two closed-throat tunnels is not good at $M = 0.80$. Comparisons were not made at higher Mach numbers since sufficient data from closed-throat tunnels are unavailable due to the inherent tunnel choking conditions.

### Comparison of Results From 6- by 19-Inch Transonic Tunnel With Theory

Two theoretical pressure distributions for inviscid potential flow for the NACA 0012 airfoil in subcritical flow have been computed and the results published in reference 13. These have been compared with the results for the present tests in figure 24. For the lifting condition good agreement between theory and experiment exists when the angle of attack, corrected for lift interference, is the same as for the theoretical case. The peak pressure at the leading edge is slightly higher for the experimental data however. For the nonlifting case good agreement exists over the airfoil.

## CONCLUDING REMARKS

The Langley 6- by 19-inch transonic tunnel was placed in operation in early 1971. This facility is a two-dimensional tunnel with top and bottom slotted walls which operates on direct blowdown from a supply of dry compressed air. The tunnel is capable of operation at Mach numbers from 0.5 to 1.1 with a corresponding Reynolds number range of about $1.5 \times 10^6$ to $3.0 \times 10^6$ based on a 10.2-cm (4.0-in.) model chord. Tunnel-empty calibrations show the local Mach number distribution obtained from wall static pressures varies less than $\pm 0.005$ from the average value in the test region occupied by the model at all Mach numbers. As part of the tunnel calibration, typical surface oil flow photographs, schlieren flow photographs, surface-pressure distributions, and integrated normal-force and pitching-moment coefficients have been obtained on an NACA 0012 airfoil section. The integrated pressure data obtained on the model have been compared with results from two other small transonic facilities and the results show that the 6- by 19-inch transonic tunnel produces slightly higher normal-force coefficients and a negative increment in pitching moment. The pressure data show this results from the fact that the shock wave on the upper surface is located farther rearward for the same Mach number and angle of attack. The data were also compared with results from two closed-throat tunnels at Mach numbers up to 0.80 and show good agreement at low angles of attack up to a Mach number of 0.70 when the data from the slotted tunnel have been corrected for lift-interference effects. As would be expected, the theoretical corrections do not give good results when large areas of supercritical flow exist on the model. When lift-

interference effects are included, good agreement between the data and two theoretical subcritical pressure distributions is also shown.

Langley Research Center,
National Aeronautics and Space Administration,
Hampton, Va., March 16, 1973.

## REFERENCES


1. Whitcomb, Richard T.; and Clark, Larry R.: An Airfoil Shape for Efficient Flight at Supercritical Mach Numbers. NASA TM X-1109, 1965.

2. Whitcomb, Richard T.; and Blackwell, James A., Jr.: Status of Research on a Supercritical Wing. Conference on Aircraft Aerodynamics, NASA SP-124, 1966, pp. 367-381.

3. Blackwell, James A., Jr.: Effect of Reynolds Number and Boundary-Layer Transition Location on Shock-Induced Separation. Transonic Aerodynamics, AGARD CP No. 35, Sept. 1968, pp. 21-1 – 21-10.

4. Blackwell, James A., Jr.: Aerodynamic Characteristics of an 11-Percent-Thick Symmetrical Supercritical Airfoil at Mach Numbers Between 0.30 and 0.85. NASA TM X-1831, 1969.

5. Jacobs, Eastman N.; Ward, Kenneth E.; and Pinkerton, Robert M.: The Characteristics of 78 Related Airfoil Sections From Tests in the Variable-Density Wind Tunnel. NACA Rep. 460, 1933.

6. Lindsey, Walter F.; and Burlock, Joseph: A 4-Microsecond Flashing Light Synchronized With Framing of Motion-Picture Cameras and Its Application in Schlieren Photography. NASA TN D-5858, 1970.

7. Gregory, N.; Quincey, V. G.; O'Reilly, C. L.; and Hall, D. J.: Progress Report on Observations of Three-Dimensional Flow Patterns Obtained During Stall Development on Aerofoils, and on the Problem of Measuring Two-Dimensional Characteristics. C.P. No. 1146, Brit. A.R.C., 1971.

8. Davis, Don D., Jr.; and Moore, Dewey: Analytical Study of Blockage- and Lift-Interference Corrections for Slotted Tunnels Obtained by the Substitution of an Equivalent Homogeneous Boundary for the Discrete Slots. NACA RM L53E07b, 1953.

9. Maeder, Paul F.; and Wood, Albert D.: Transonic Wind Tunnel Test Sections. Z. Angew. Math. Phys., vol. VII, fasc. 3, May 25, 1956, pp. 177-212.

10. Ladson, Charles L.: Two-Dimensional Airfoil Characteristics of Four NACA 6A-Series Airfoils at Transonic Mach Numbers up to 1.25. NACA RM L57F05, 1957.

11. Carpenter, Paul J.: Lift and Profile-Drag Characteristics of an NACA-0012 Airfoil Section as Derived From Measured Helicopter-Rotor Hovering Performance. NACA TN 4357, 1958.

12. Lizak, Alfred A.: Two-Dimensional Wind-Tunnel Tests of an H-34 Main Rotor Airfoil Section. TREC Tech. Rep. 60-53 (SER-58304), U.S. Army Transportation Res. Command (Fort Eustis, Va.), Sept. 1960.

13. Lock, R. C.: Test Cases for Numerical Methods in Two-Dimensional Transonic Flows. AGARD Rep. No. 575, Nov. 1970.

TABLE I.- NACA 0012 ORDINATES

[All dimensions are in percent]

| Theory | | Measured | |
|---|---|---|---|
| $\frac{x}{c}$ (a) | $\frac{y}{c}$ | $\frac{y_{upper}}{c}$ | $\frac{y_{lower}}{c}$ |
| 0 | 0 | ----- | ----- |
| 1.25 | 1.894 | 1.905 | 1.929 |
| 2.5 | 2.615 | 2.704 | 2.709 |
| 5.0 | 3.555 | 3.633 | 3.628 |
| 7.5 | 4.200 | 4.264 | 4.246 |
| 10.0 | 4.683 | 4.756 | 4.729 |
| 15.0 | 5.345 | 5.409 | 5.363 |
| 20.0 | 5.738 | 5.779 | 5.723 |
| 25.0 | 5.941 | 5.975 | 5.904 |
| 30.0 | 6.002 | 6.018 | 5.916 |
| 40.0 | 5.803 | 5.845 | 5.771 |
| 50.0 | 5.294 | 5.356 | 5.275 |
| 60.0 | 4.563 | 4.619 | 4.540 |
| 70.0 | 3.664 | 3.710 | 3.633 |
| 80.0 | 2.623 | 2.664 | 2.598 |
| 90.0 | 1.448 | 1.459 | 1.418 |
| 95.0 | .807 | .811 | .778 |
| 100.0 | .126 | .168 | .131 |

[a]Measured values are the same.

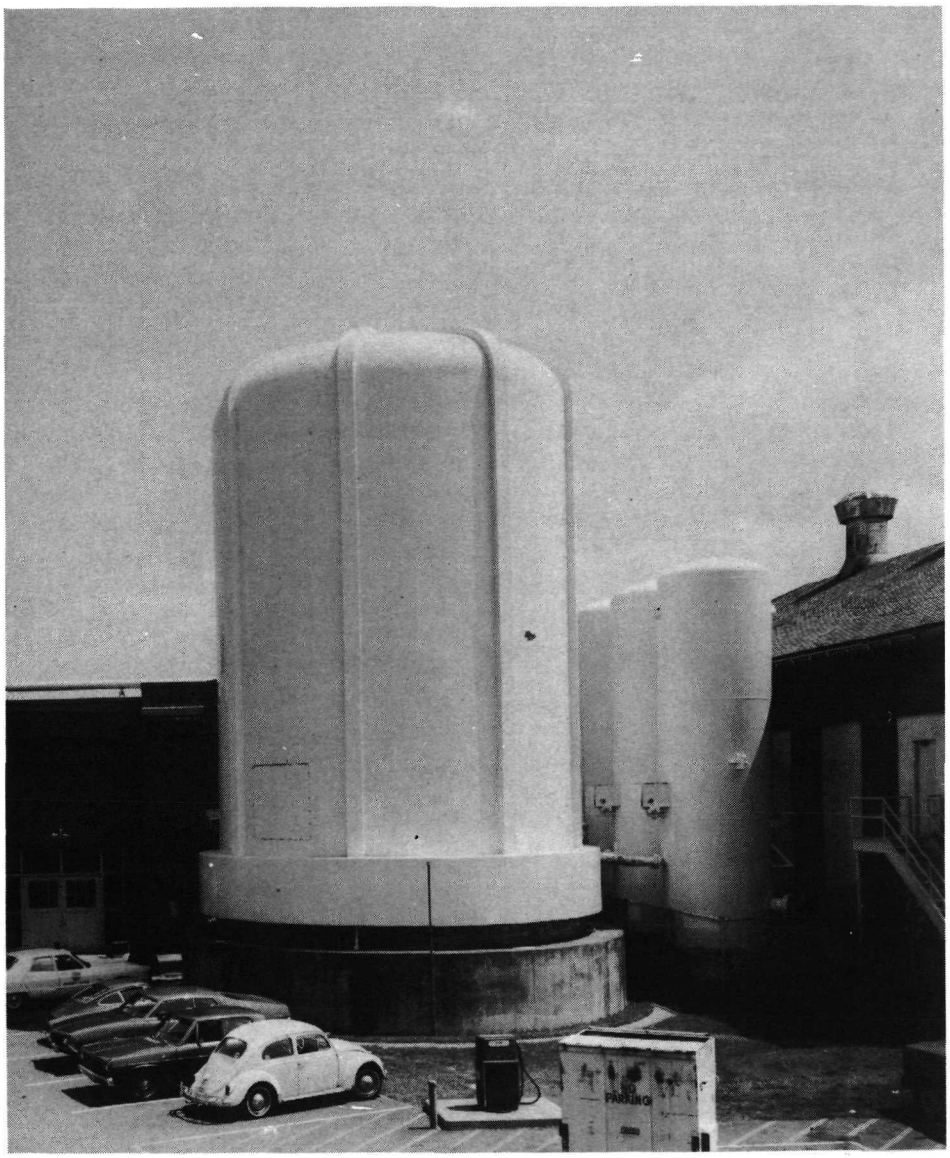

L-73-299

(a) Exterior view.

Figure 1.- Photograph of the Langley 6- by 19-inch transonic tunnel.

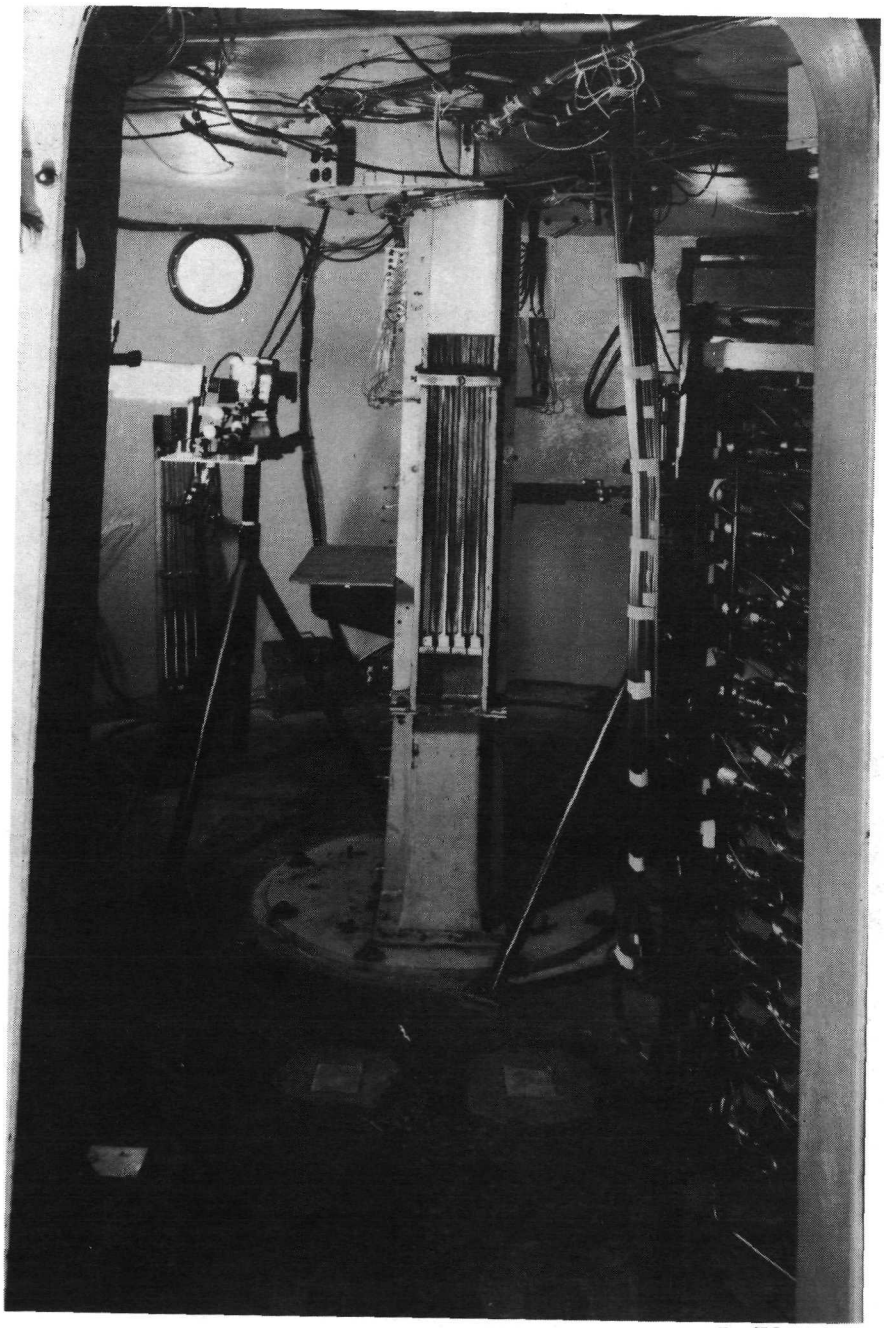

L-72-6127

(b) Interior view.

Figure 1.- Concluded.

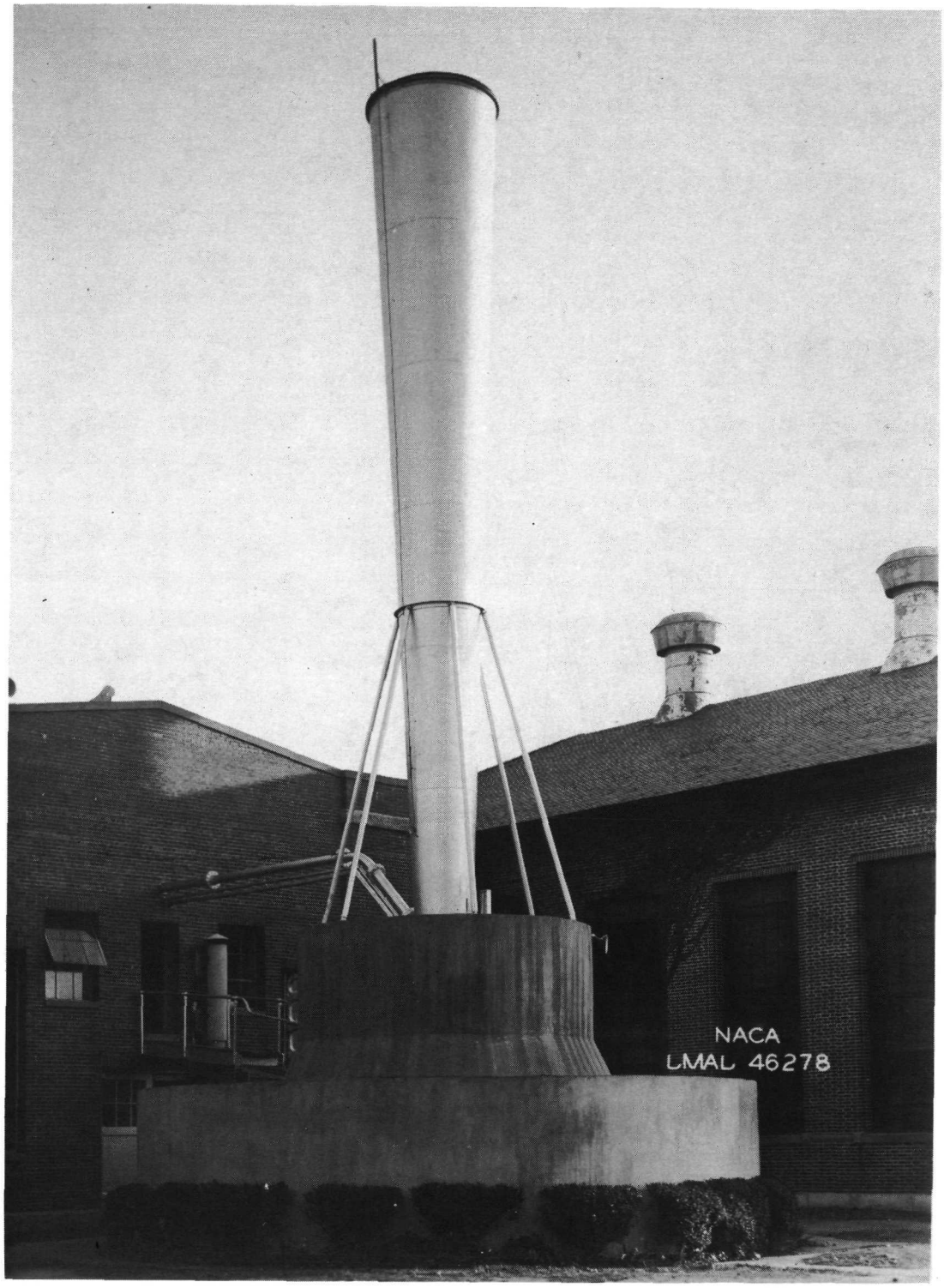


(a) Exterior photograph.

Figure 2.- The Langley 24-inch high-speed tunnel.

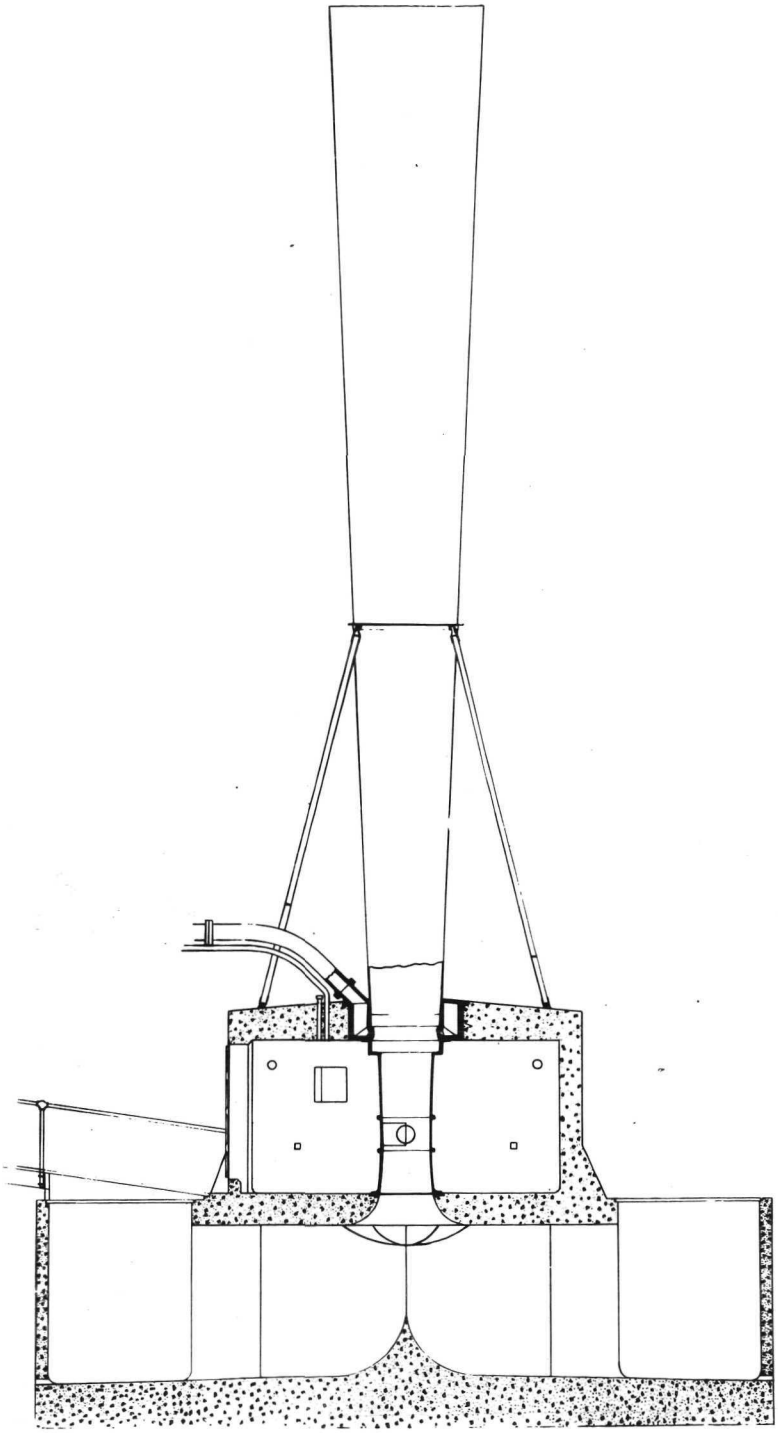

(b) Cross-section drawing.

Figure 2.- Concluded.

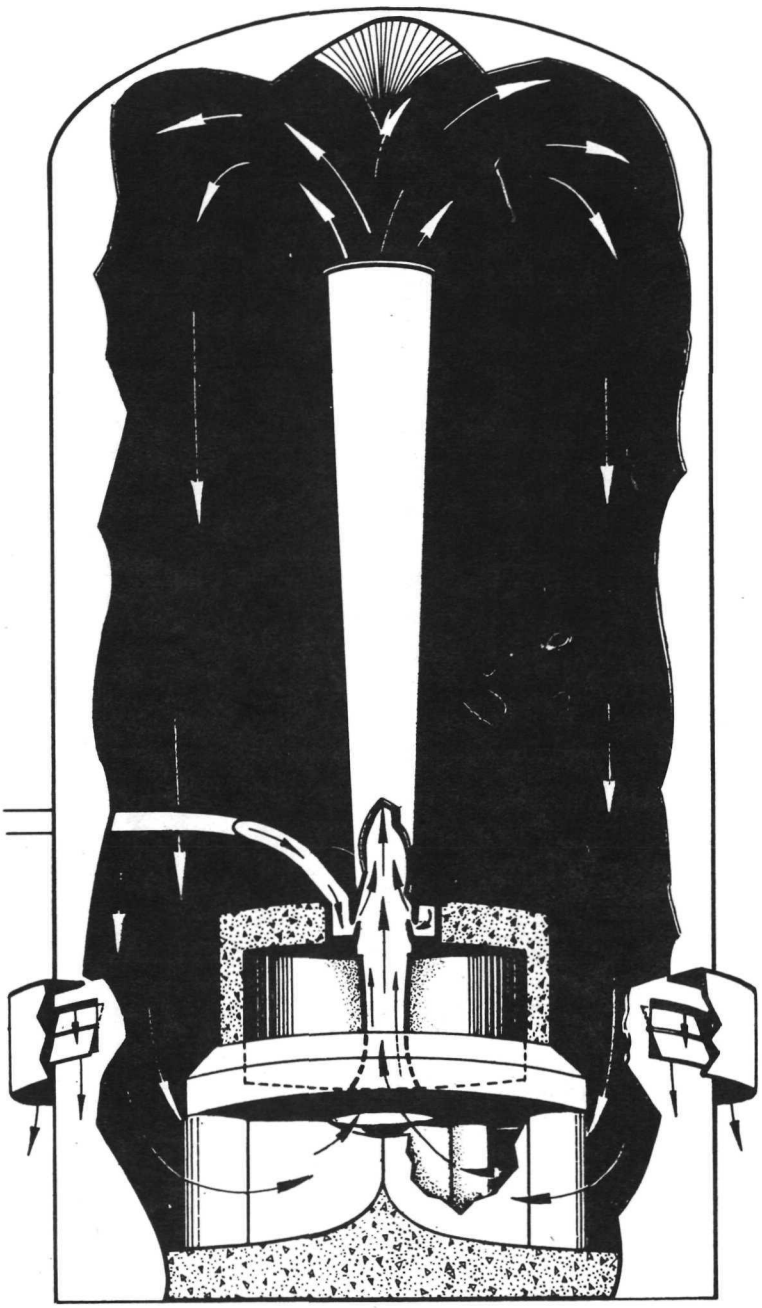

Figure 3.- Enclosure around Langley 24-inch high-speed tunnel.

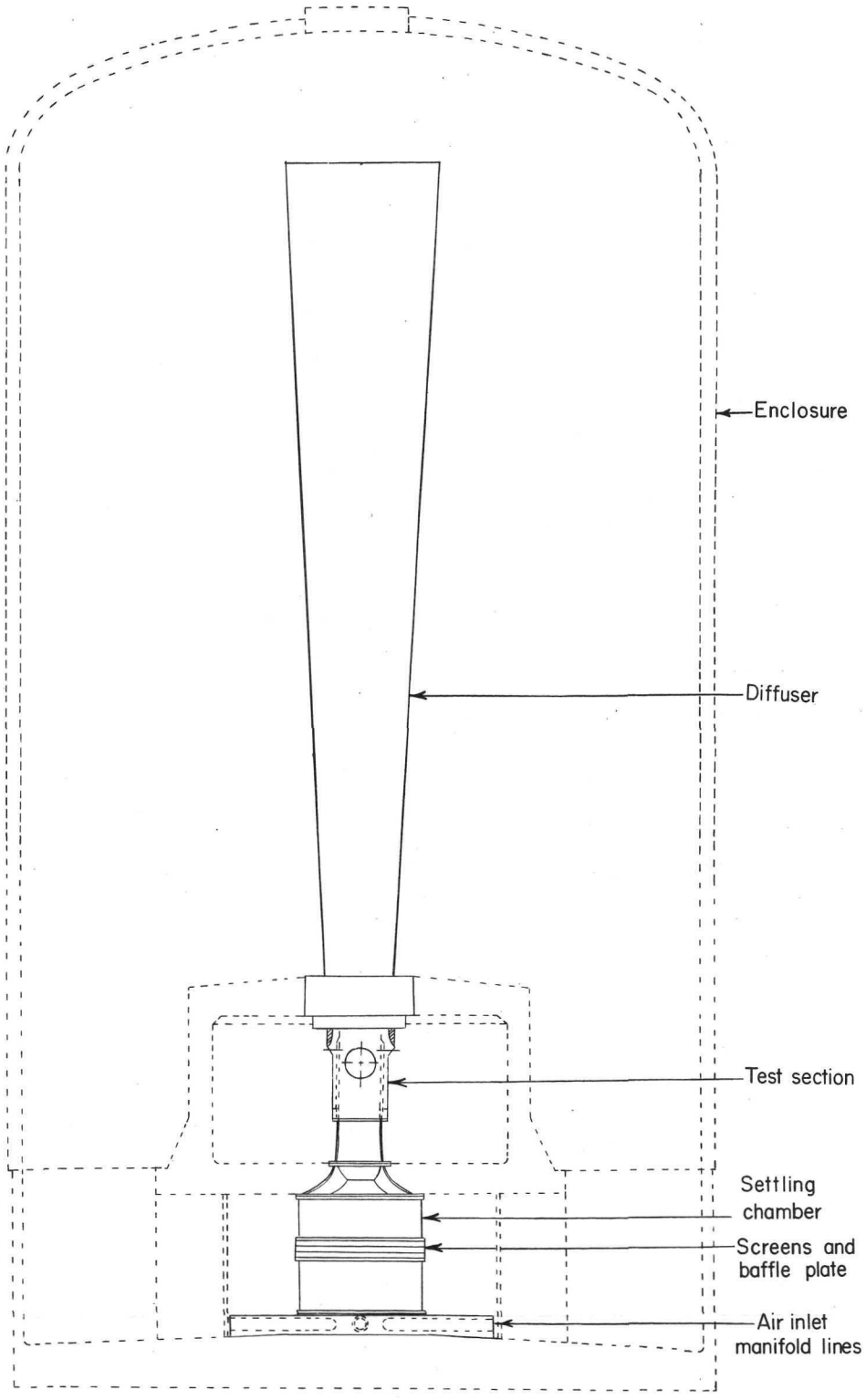


(a) Overall view.

Figure 4.- Cross-section drawings of the Langley 6- by 19-inch transonic tunnel.

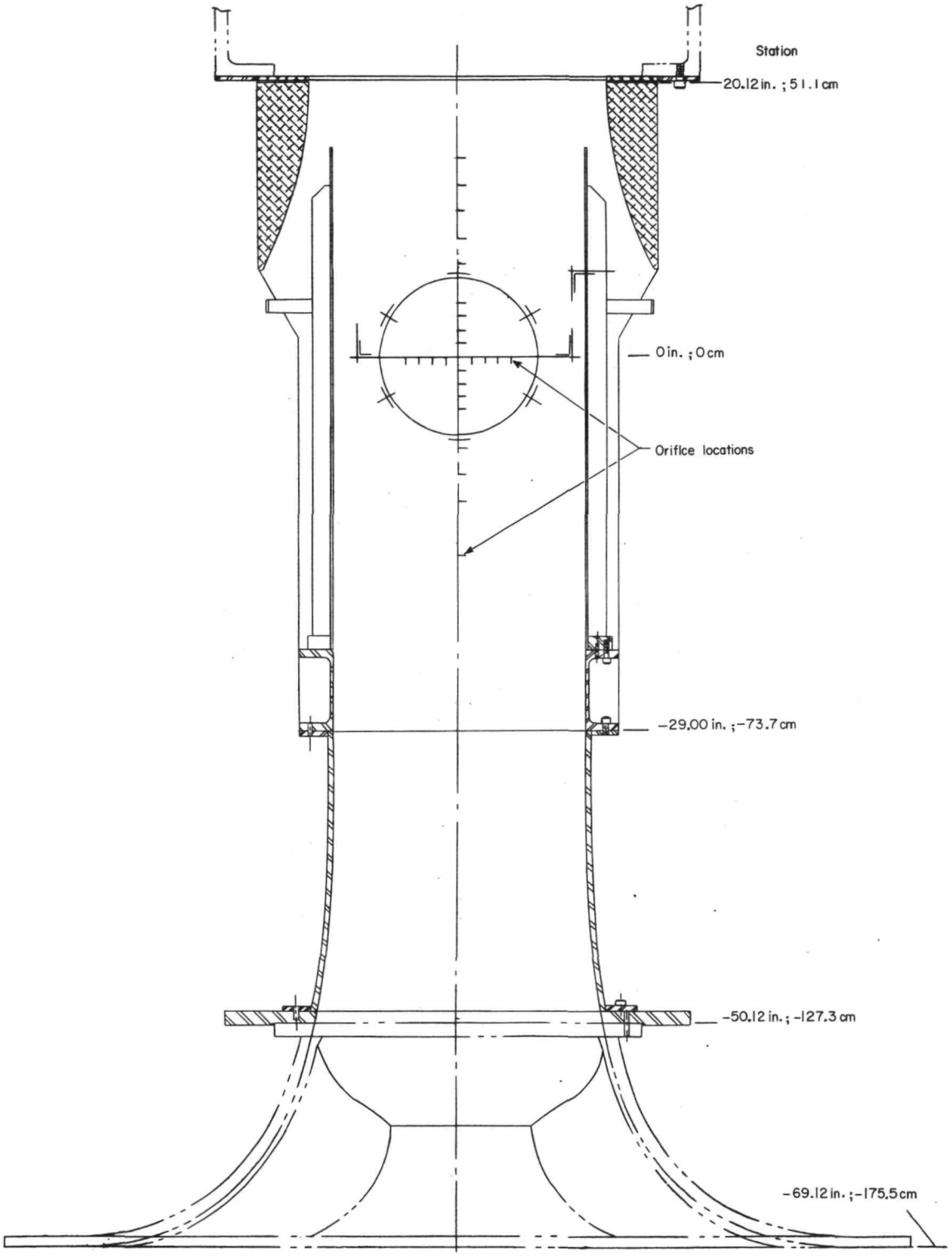


(b) Test-section details.

Figure 4.- Continued.

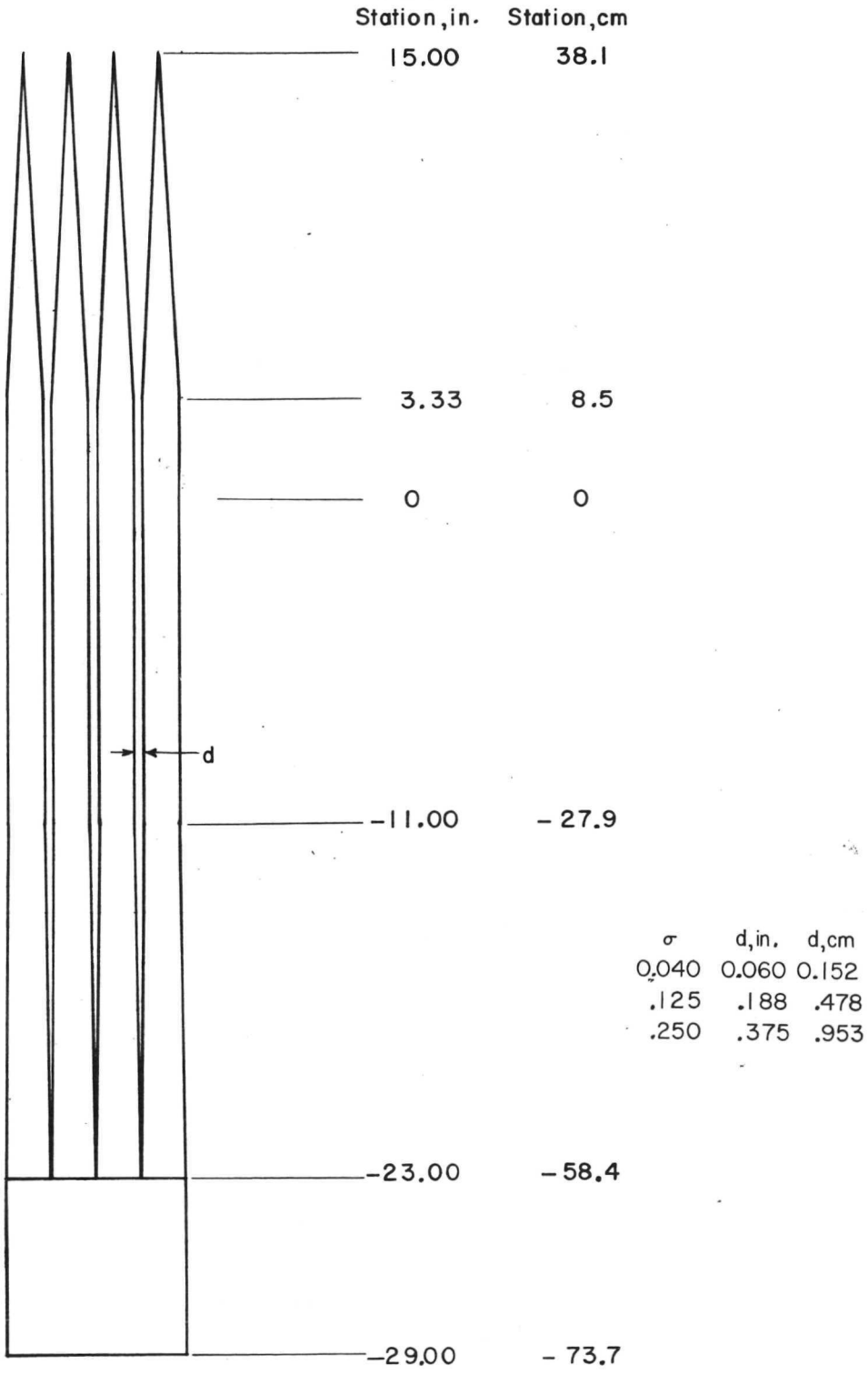


| σ | d, in. | d, cm |
|---|---|---|
| 0.040 | 0.060 | 0.152 |
| .125 | .188 | .478 |
| .250 | .375 | .953 |

(c) Details of slotted walls.

Figure 4.- Concluded.

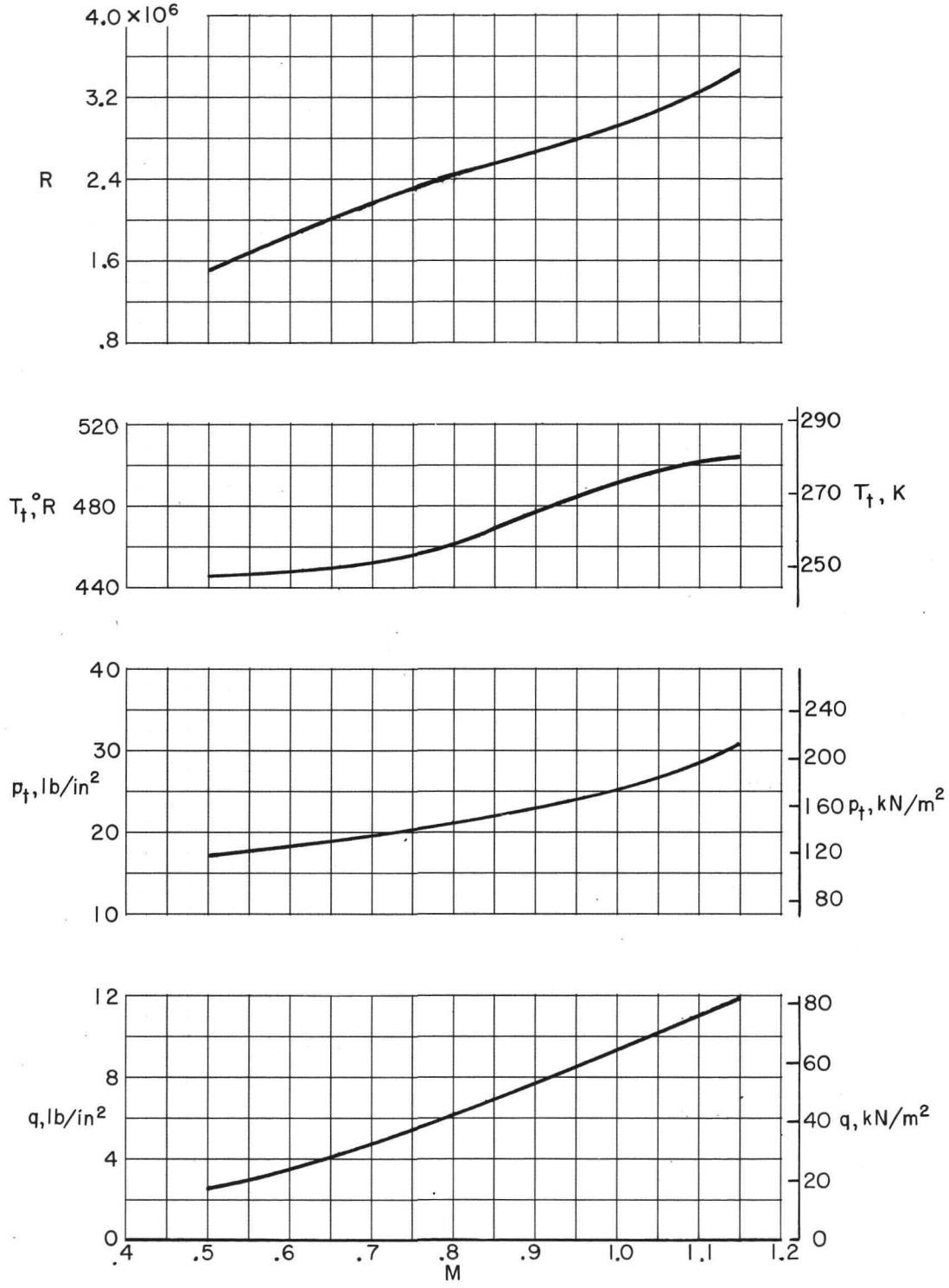


Figure 5.- Typical operational characteristics of the 6- by 19-inch transonic tunnel.

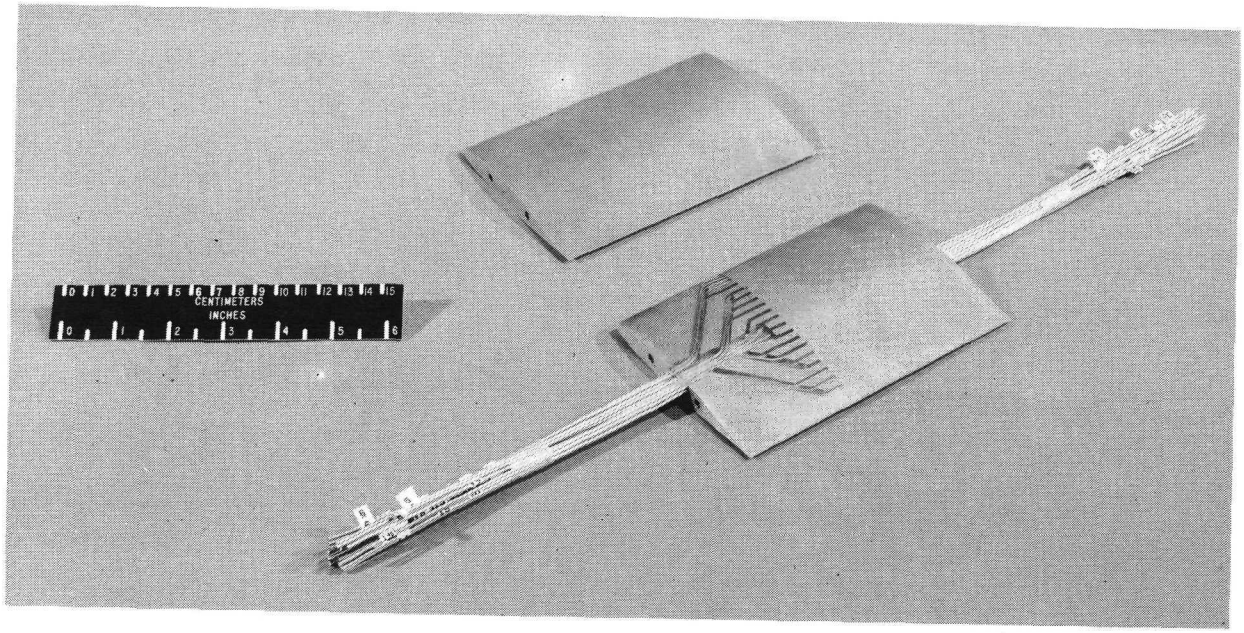


L-72-4711

TYPICAL ORIFICE LOCATIONS

| x/c | x/c |
|---|---|
| 0.0125 | 0.45 |
| .025 | .50 |
| .05 | .55 |
| .075 | .60 |
| .10 | .65 |
| .15 | .70 |
| .20 | .75 |
| .25 | .80 |
| .30 | .85 |
| .35 | .90 |
| .40 | .95 |

Figure 6.- Photograph of typical schlieren and pressure-distribution models. c = 10.2 cm (4.0 in.).

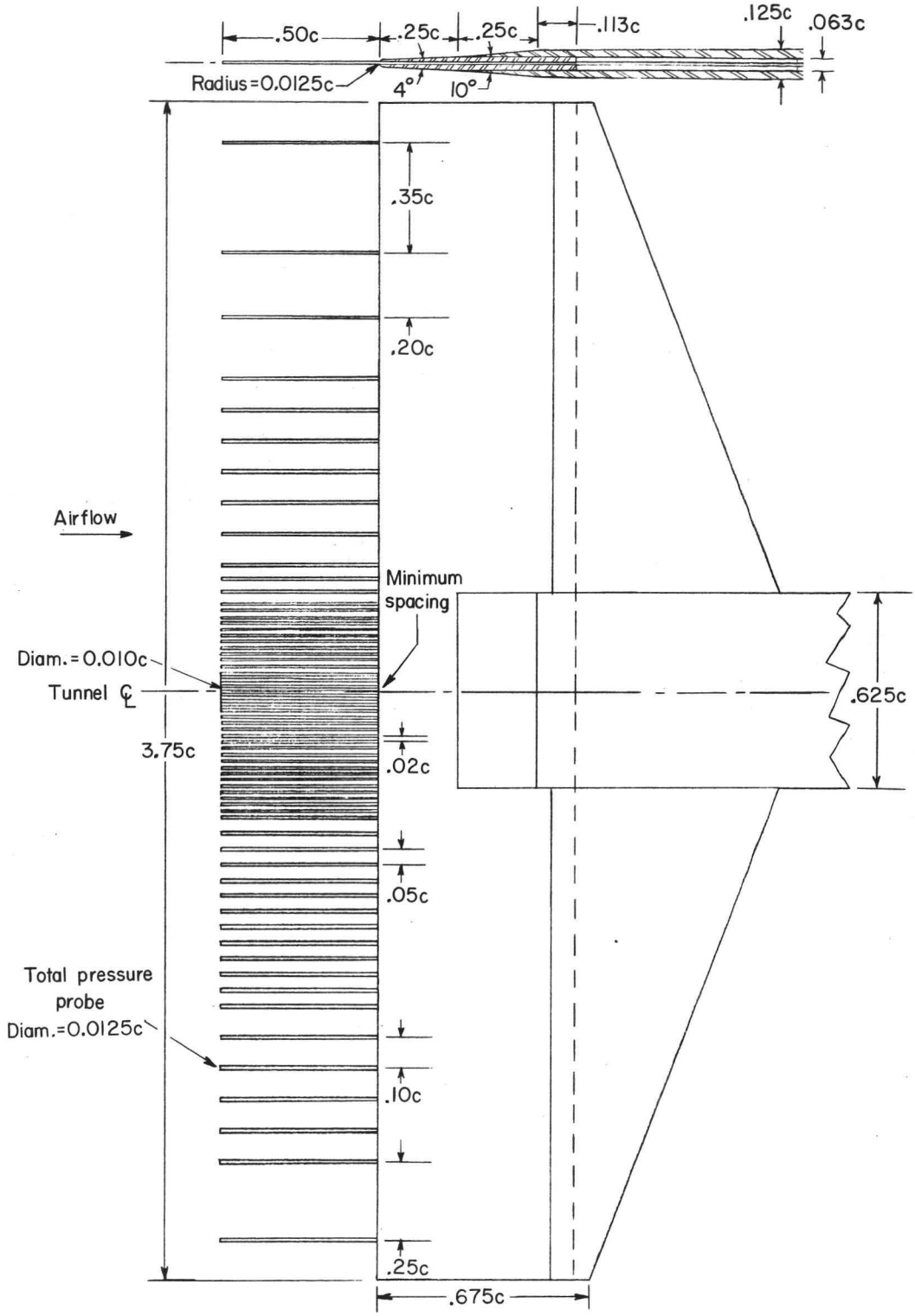


Figure 7.- Detail drawing of the wake survey rake. c = 10.2 cm (4.0 in.).

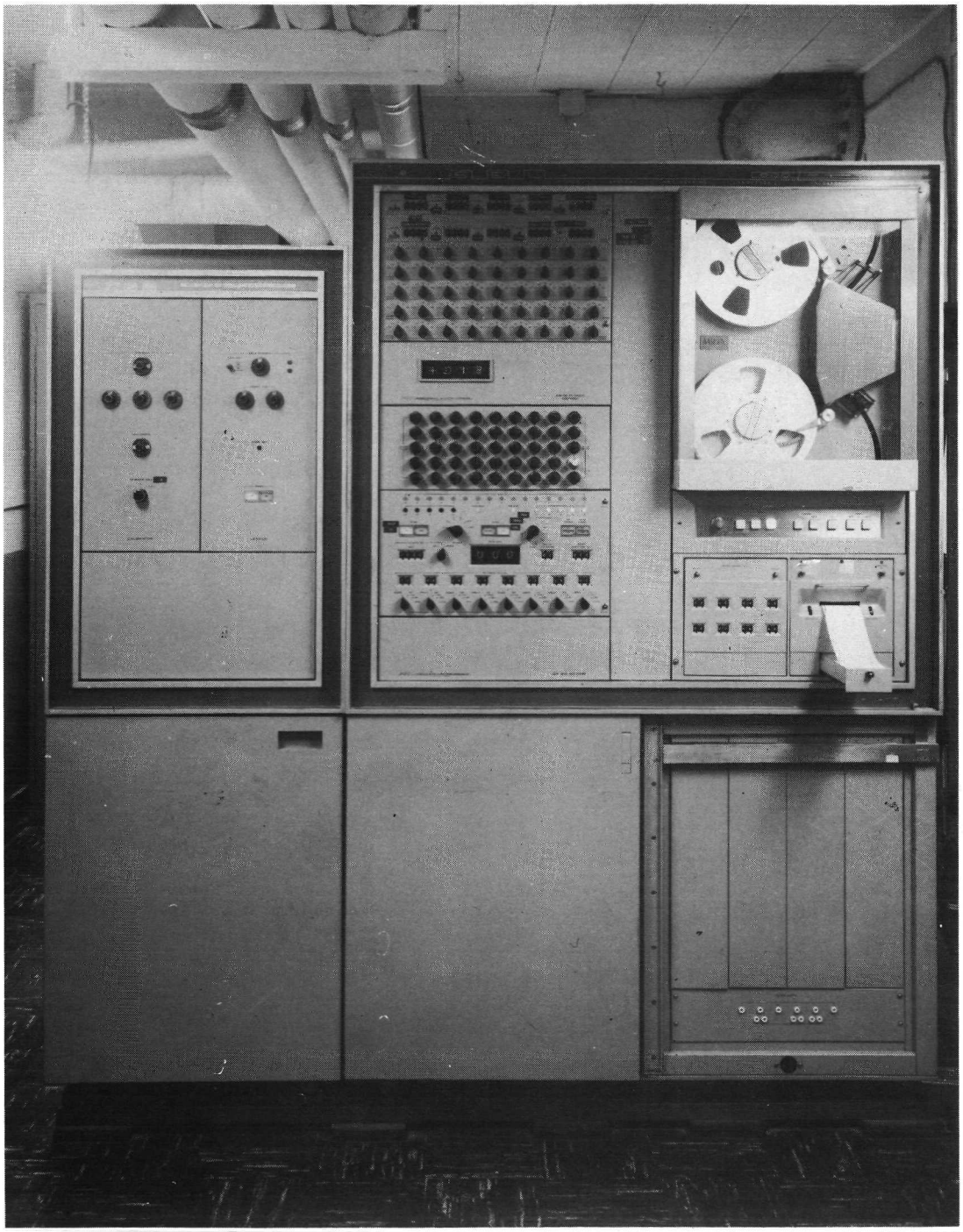

L-72-876

(a) Data acquisition system.

Figure 8.- Photograph of control room of Langley 6- by 19-inch transonic tunnel.

L-72-877

(b) Control console.

Figure 8.- Concluded.

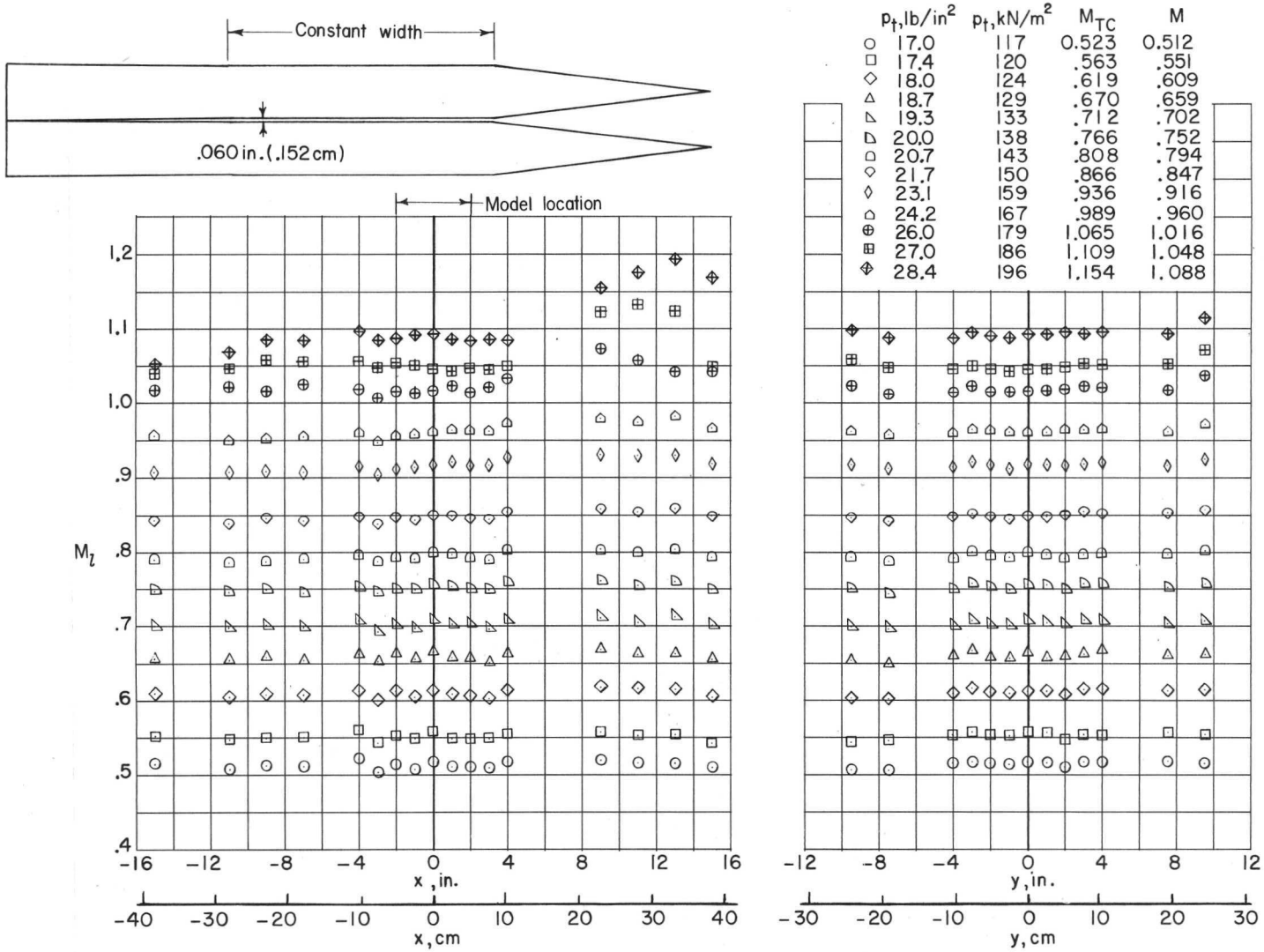


(a) Longitudinal (y = 0). (b) Vertical (x = 0).

Figure 9.- Mach number distribution in the Langley 6- by 19-inch transonic tunnel, tunnel empty. $\sigma = 0.040$.

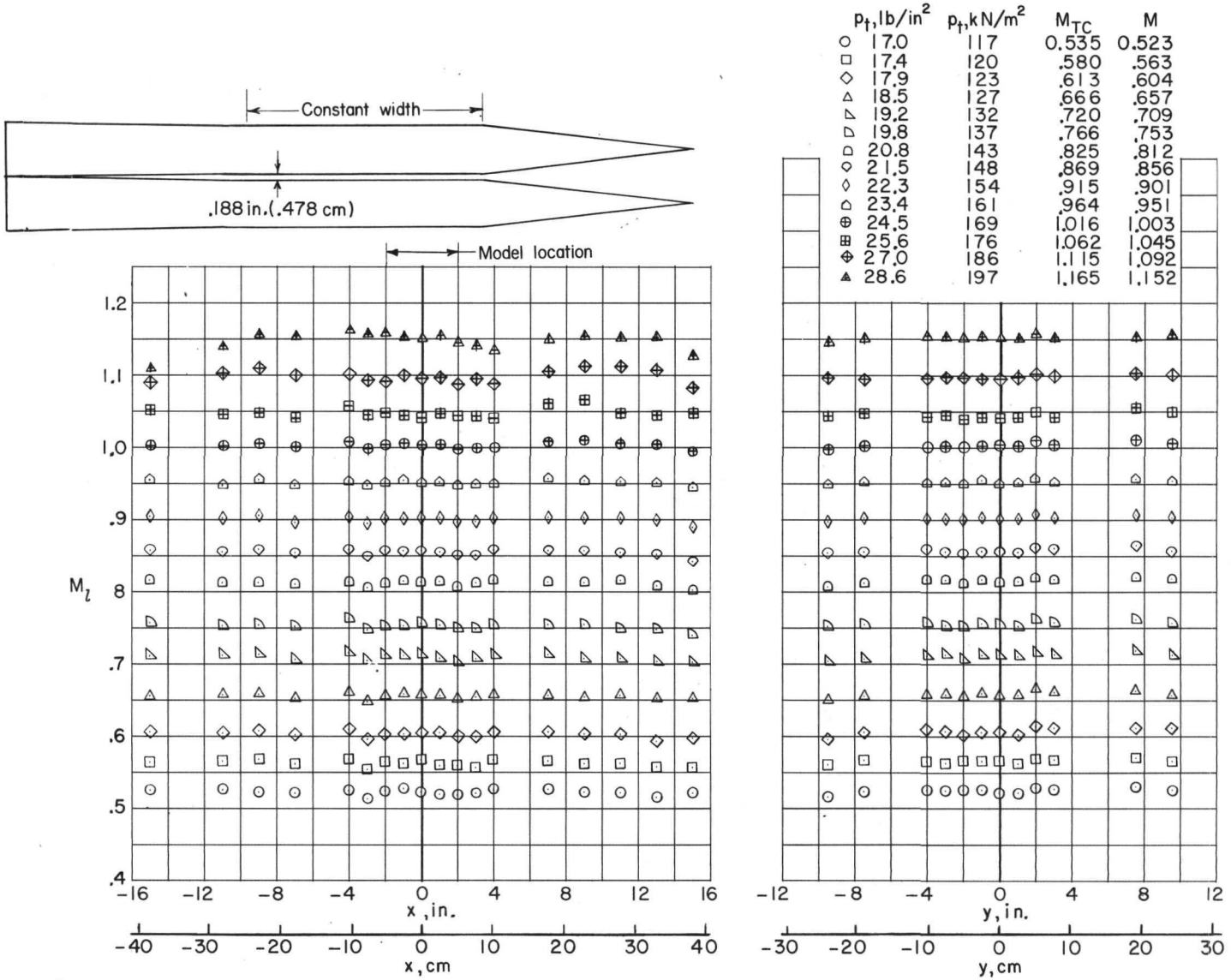


(a) Longitudinal (y = 0).

(b) Vertical (x = 0).

Figure 10.- Mach number distribution in the Langley 6- by 19-inch transonic tunnel, tunnel empty. $\sigma = 0.125$.

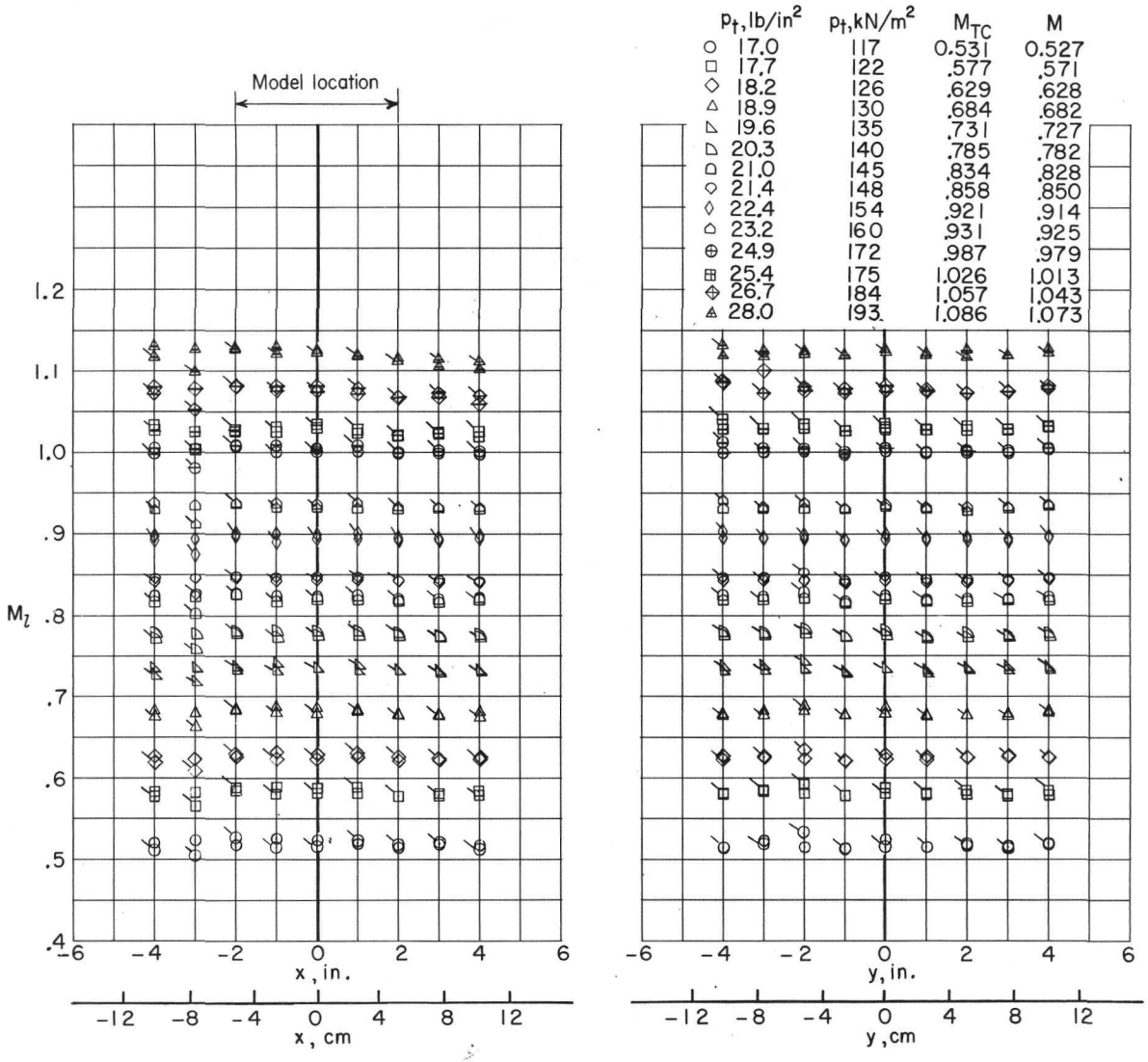


Figure 11.- Comparison of Mach number distribution on left- and right-hand walls of the Langley 6- by 19-inch transonic tunnel, tunnel empty. $\sigma = 0.125$. Flagged symbols are for right-hand wall.

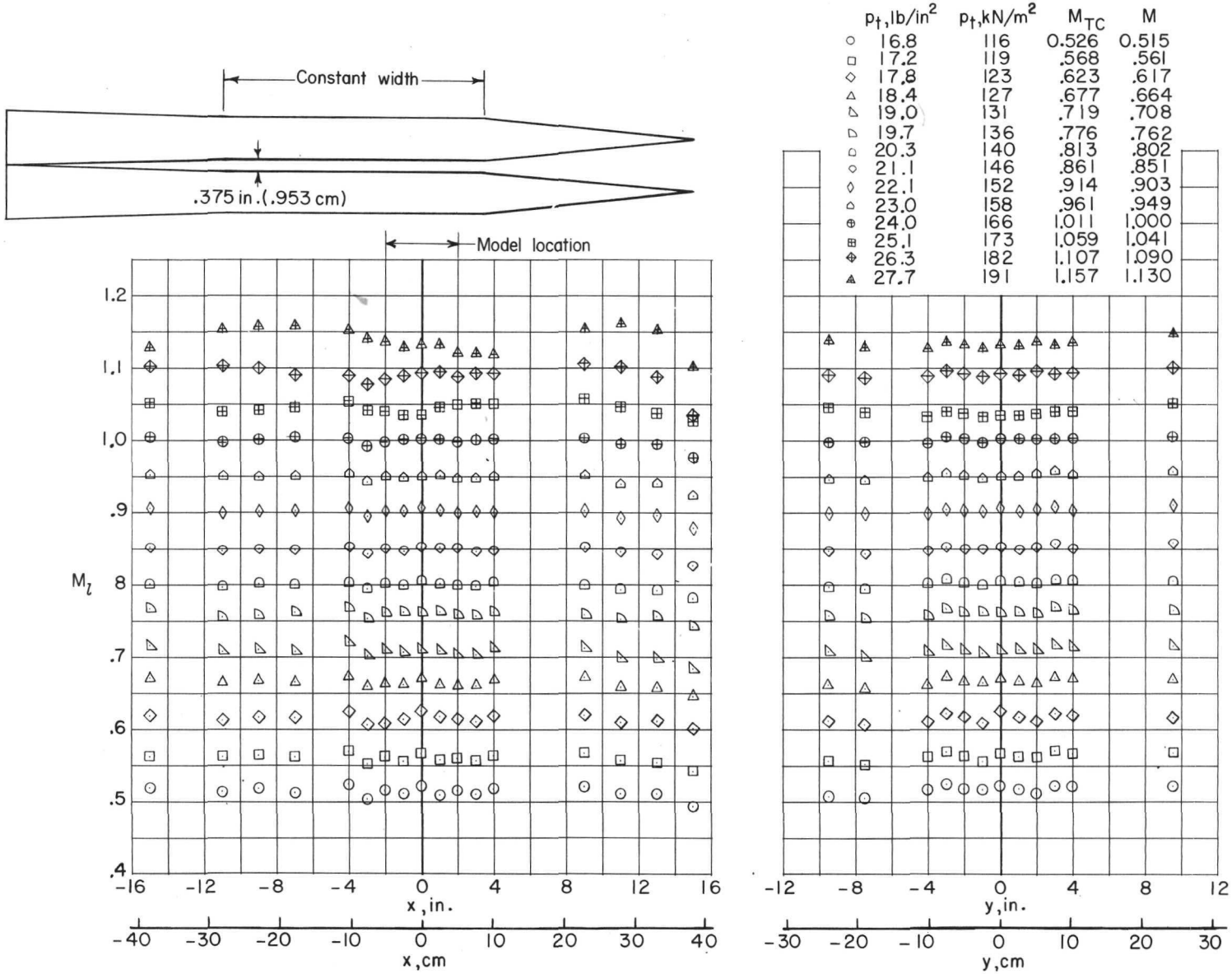


(a) Longitudinal (y = 0).

(b) Vertical (x = 0).

Figure 12.- Mach number distribution in the Langley 6- by 19-inch transonic tunnel, tunnel empty. $\sigma = 0.250$.

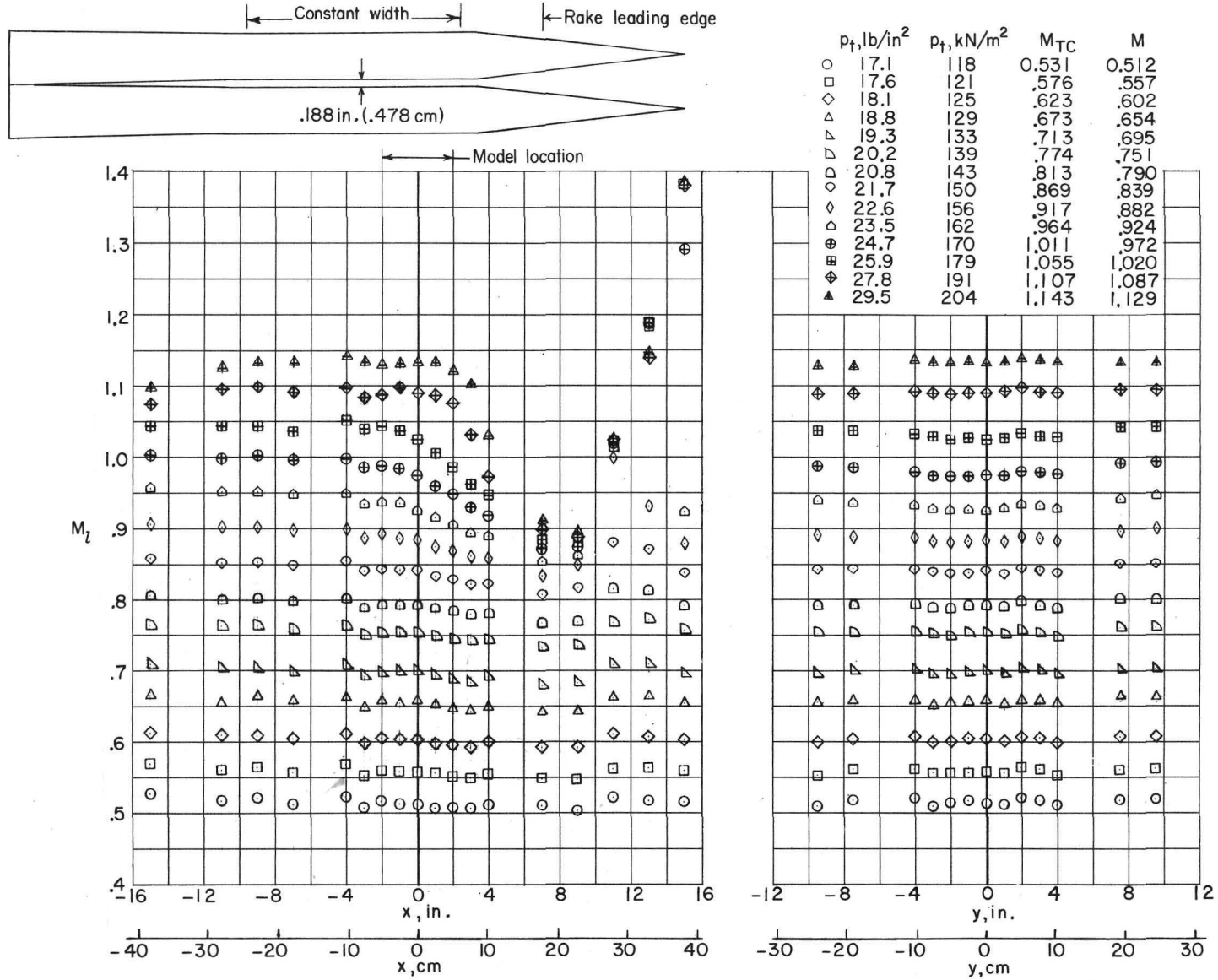


(a) Longitudinal (y = 0). (b) Vertical (x = 0).

Figure 13.- Mach number distribution in the Langley 6- by 19-inch transonic tunnel, with rake. $\sigma = 0.125$.

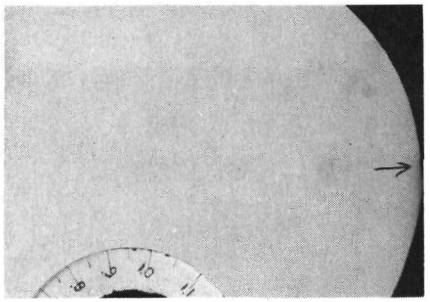

M = 0

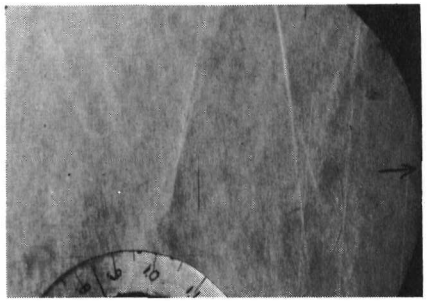

M = 0.85

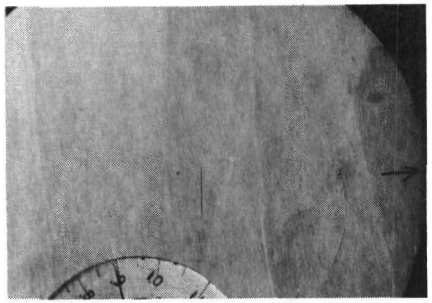

M = 0.90

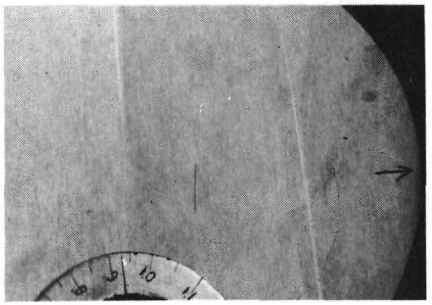

M = 0.93

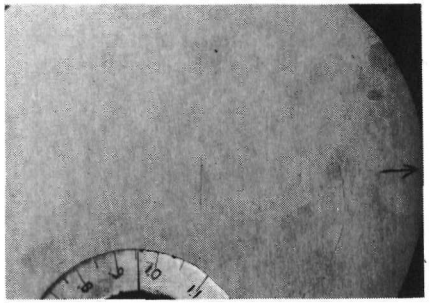

M = 0.95

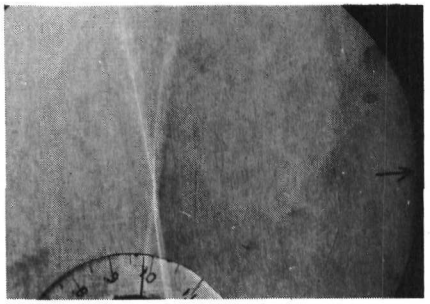

M = 0.98

M = 1.00

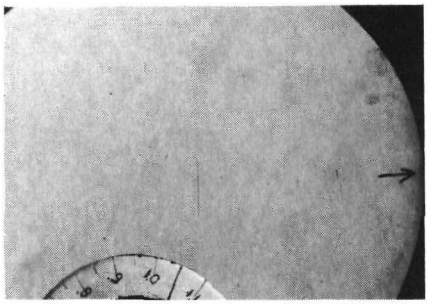

M = 1.05

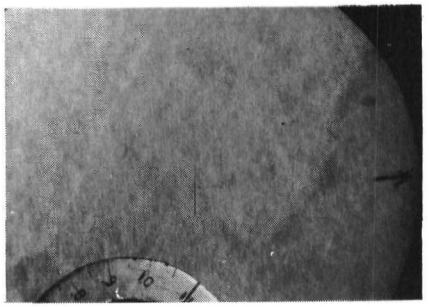

M = 1.10

(a) Without rake.

L-73-300

Figure 14.- Schlieren flow photographs of empty 6- by 19-inch transonic tunnel.

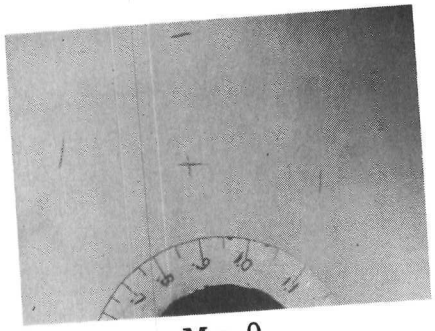
M = 0

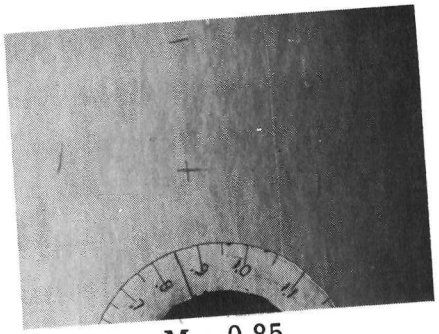
M = 0.85

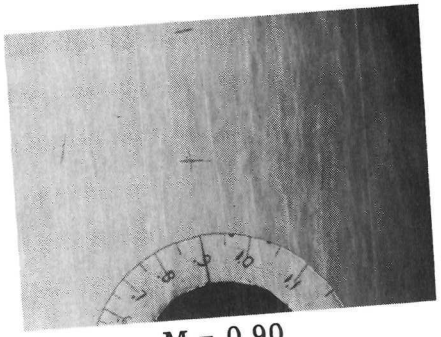
M = 0.90

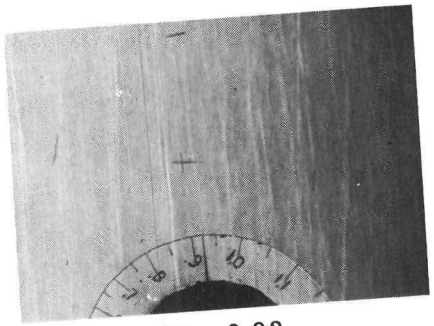
M = 0.93

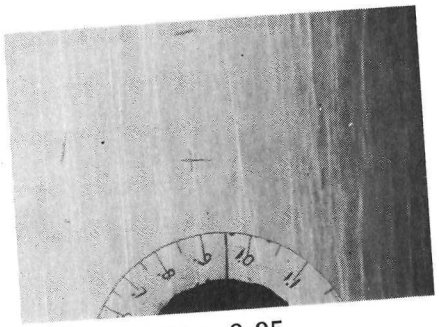
M = 0.95

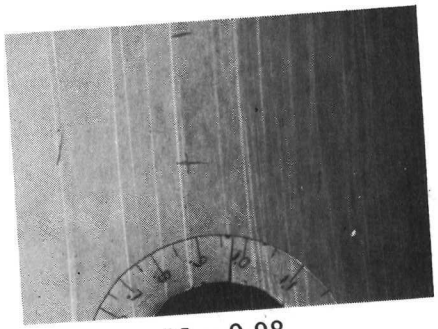
M = 0.98

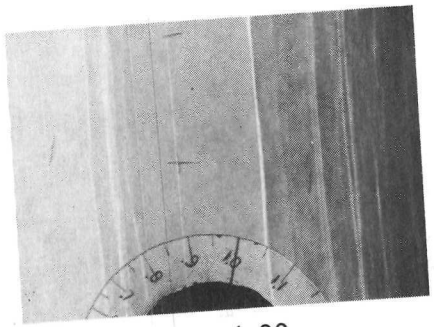
M = 1.00

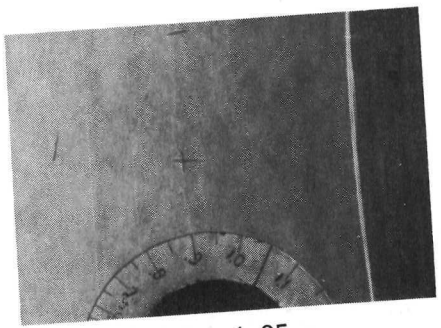
M = 1.05

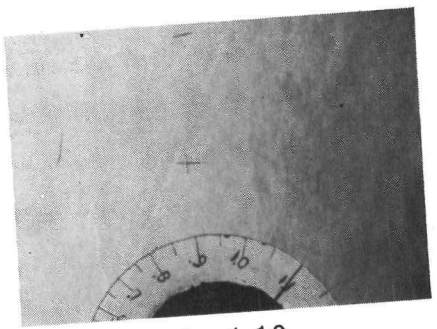
M = 1.10

L-73-3001

(b) With wake survey rake.

Figure 14.- Concluded.

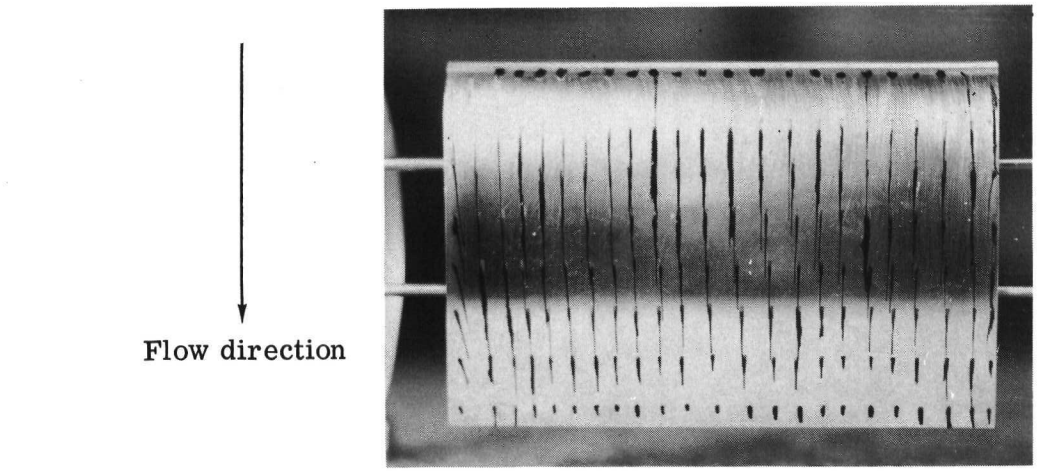


$\alpha = 8^{o}$

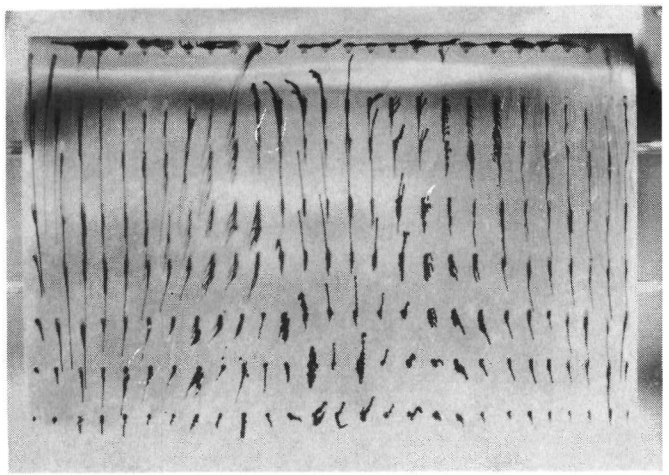

$\alpha = 10^{o}$

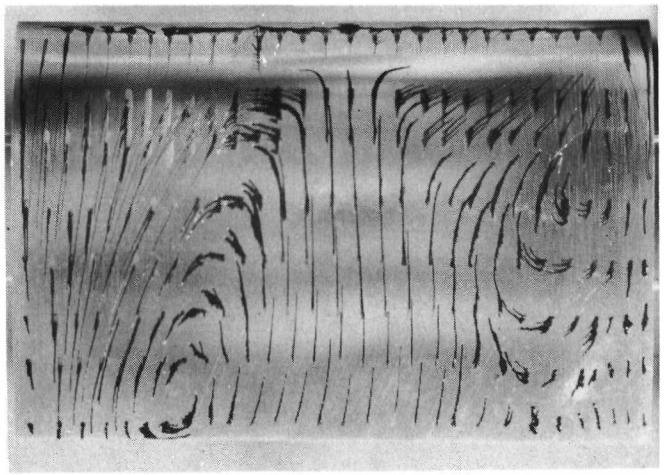

$\alpha = 12^{o}$

(a) M = 0.50.

L-73-3002

Figure 15.- Surface oil flow patterns on NACA 0012 airfoil section.

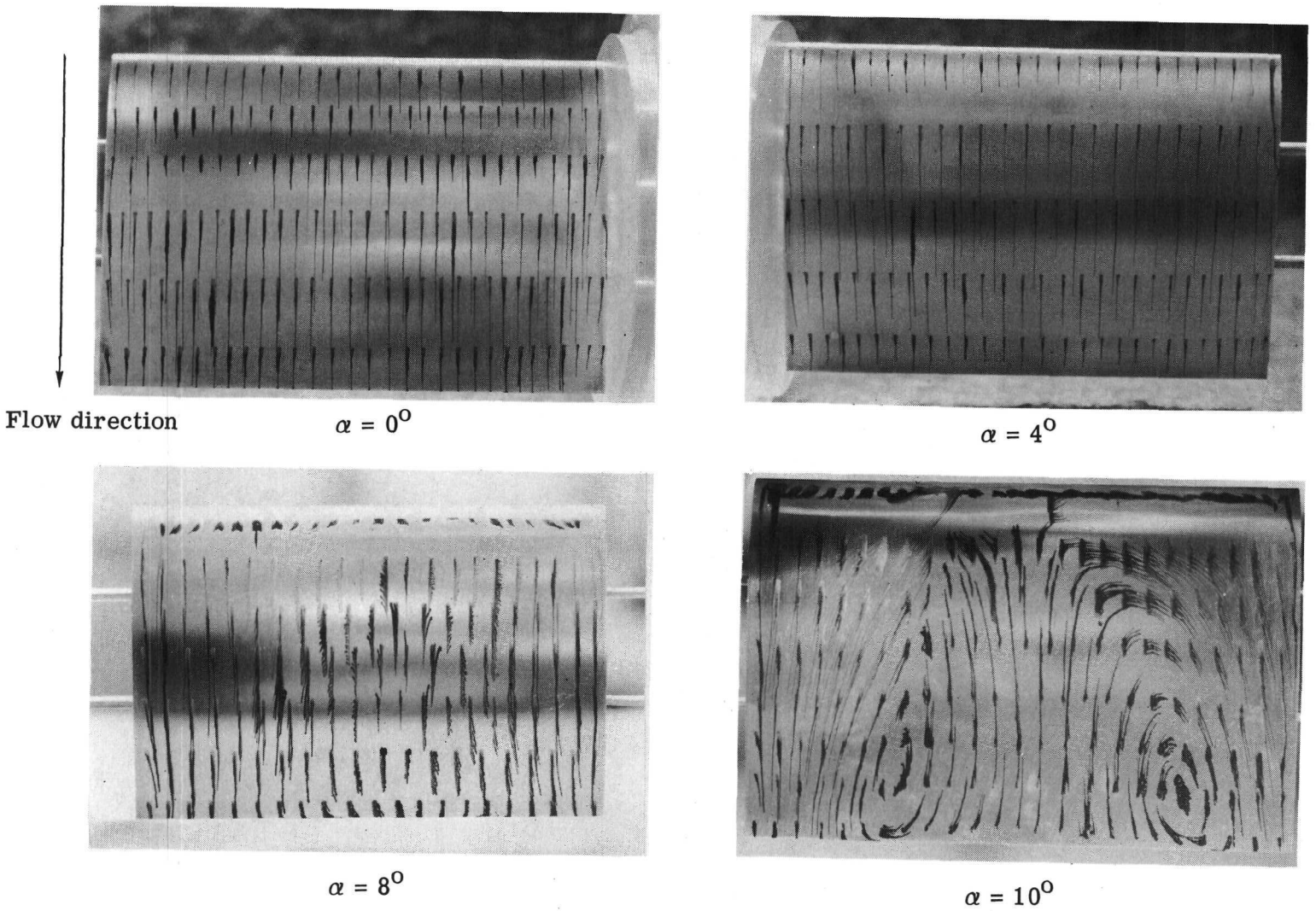


(b) M = 0.65.

L-73-3003

Figure 15.- Concluded.

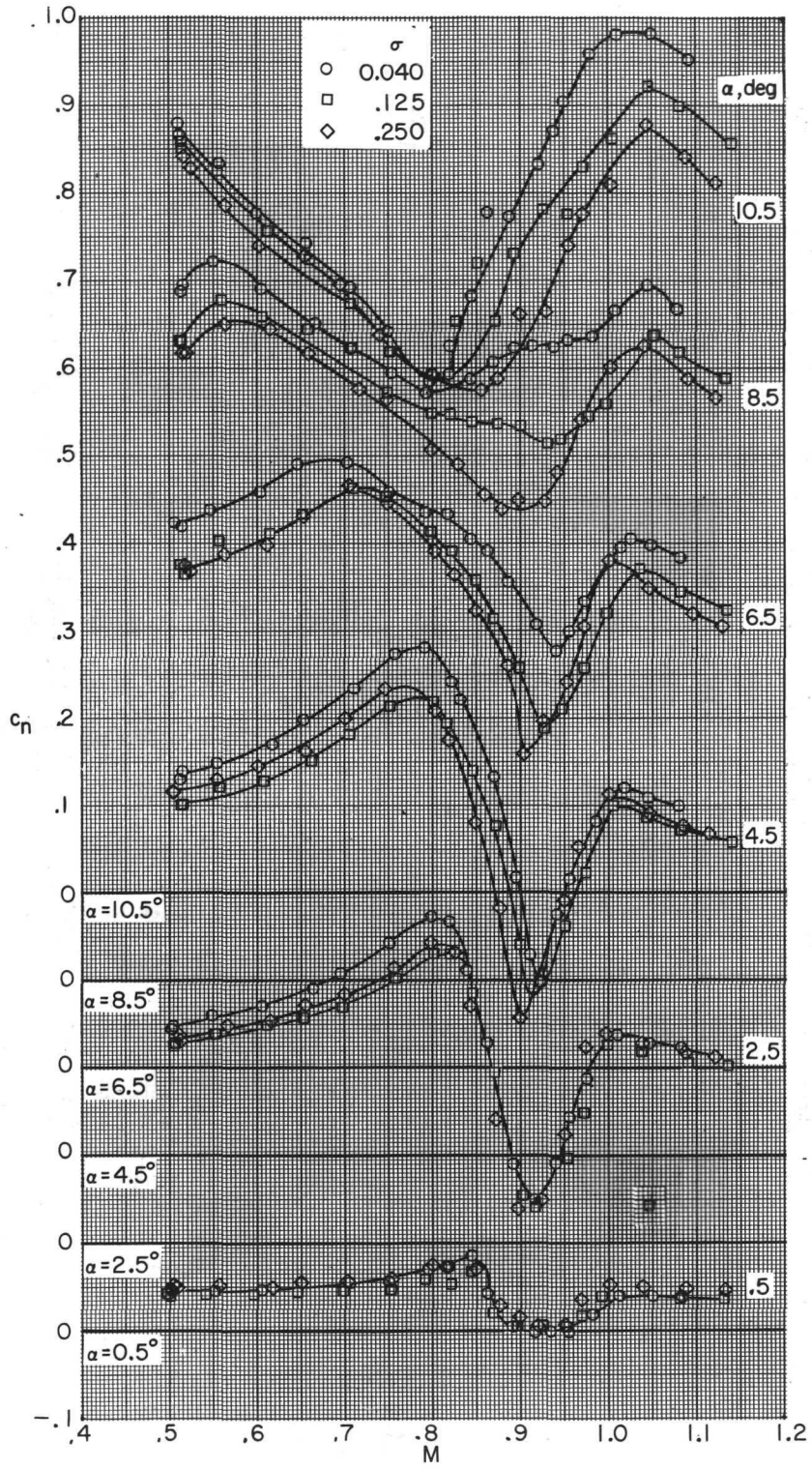


(a) Normal-force coefficient.

Figure 16.- Effects of wall open area ratio on aerodynamic characteristics of the NACA 0012 airfoil section.

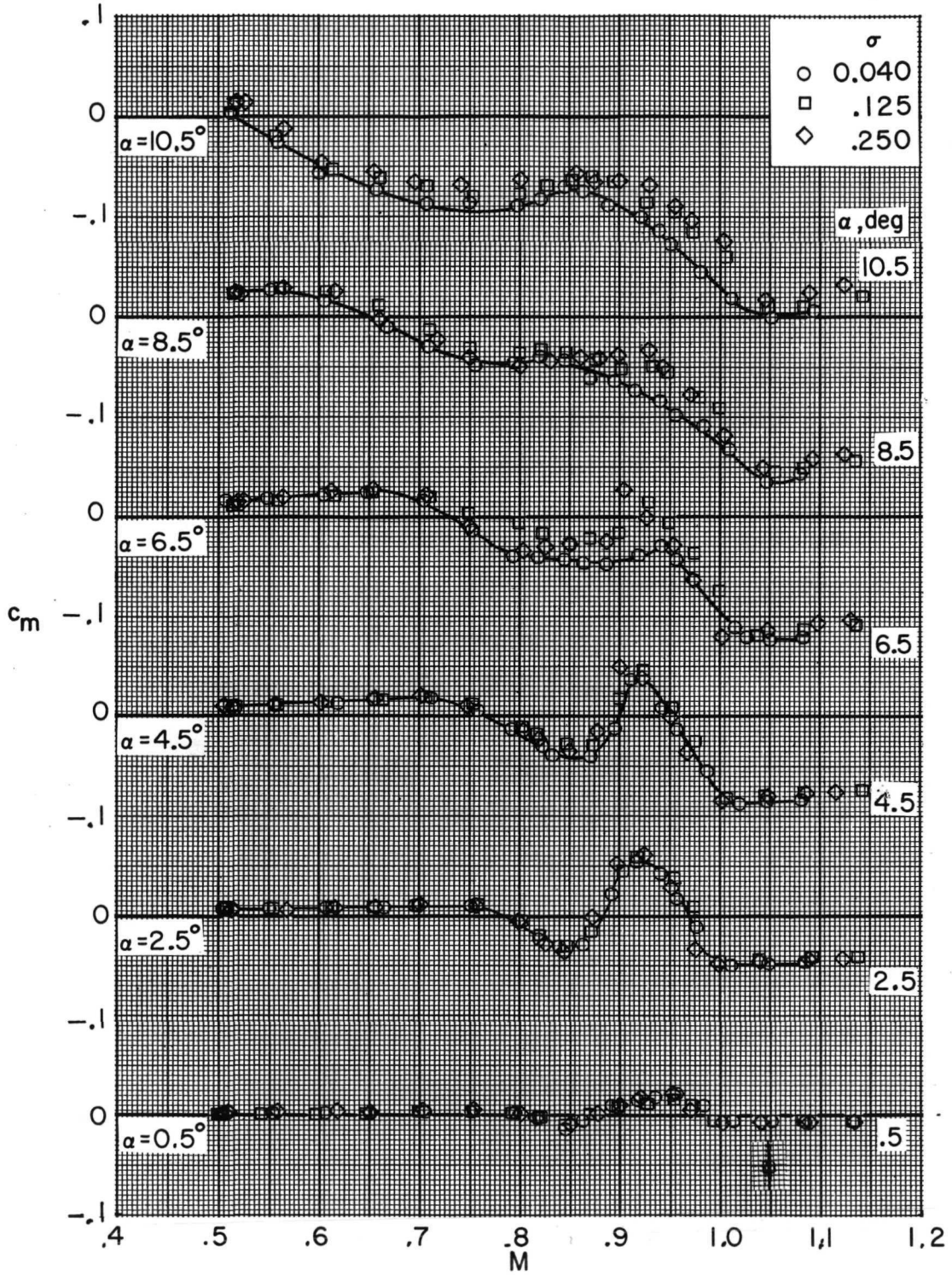


(b) Pitching-moment coefficient.

Figure 16.- Concluded.

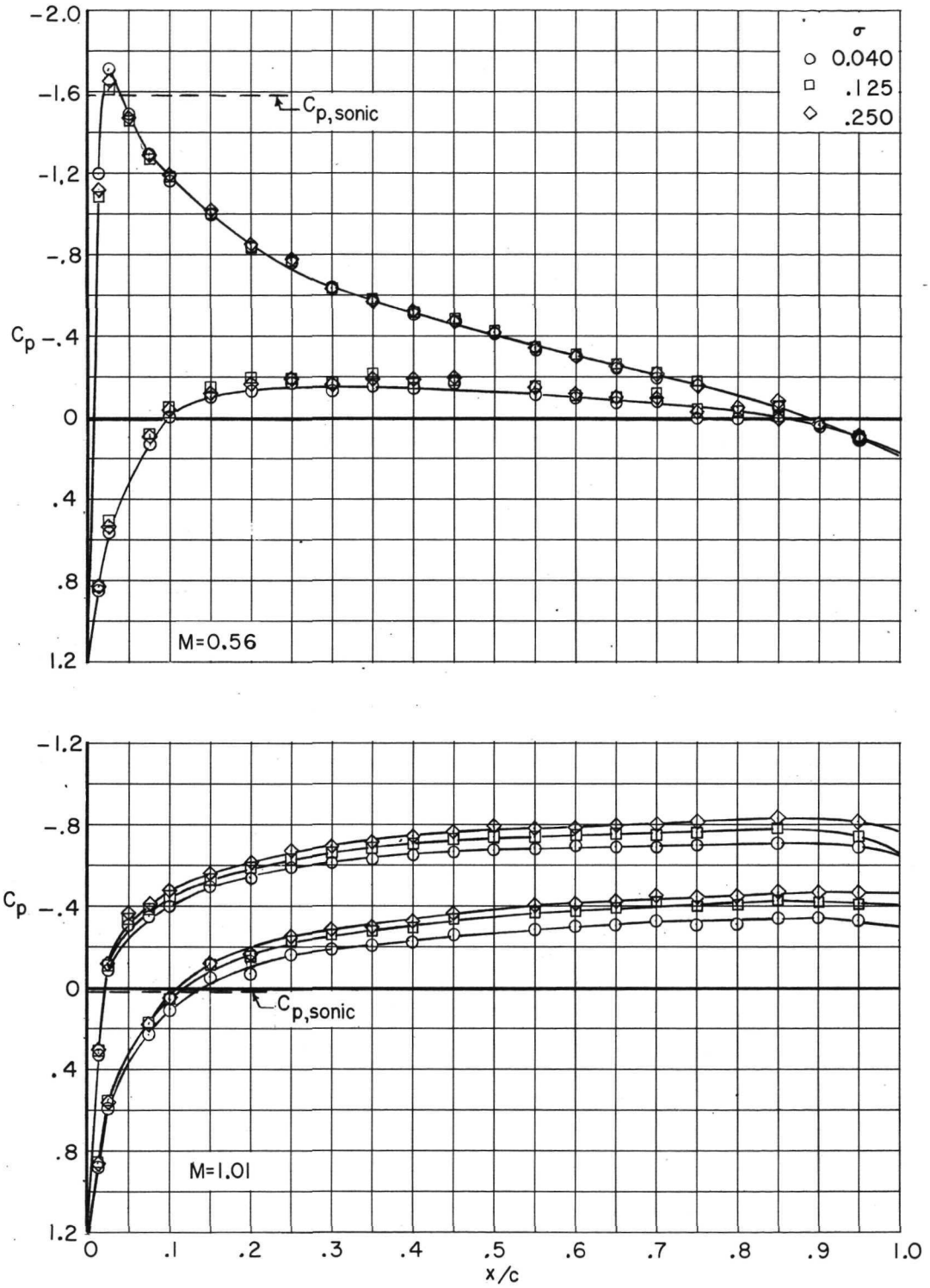


(a) $\alpha = 4.5^{o}$.

Figure 17.- Effects of wall open area ratio on pressure distributions over the NACA 0012 airfoil section.

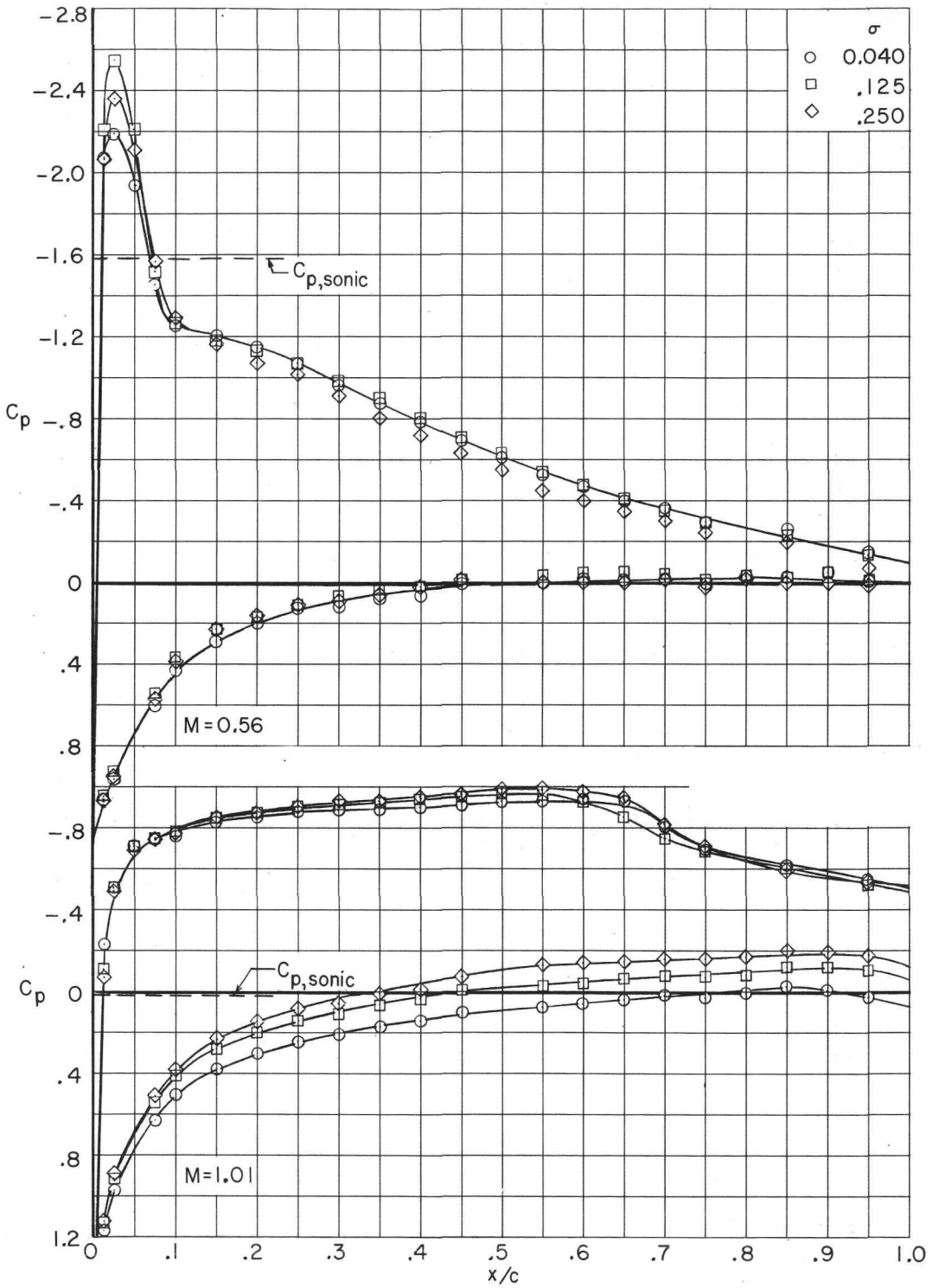


(b) $\alpha = 10.5^{o}$.

Figure 17.- Concluded.

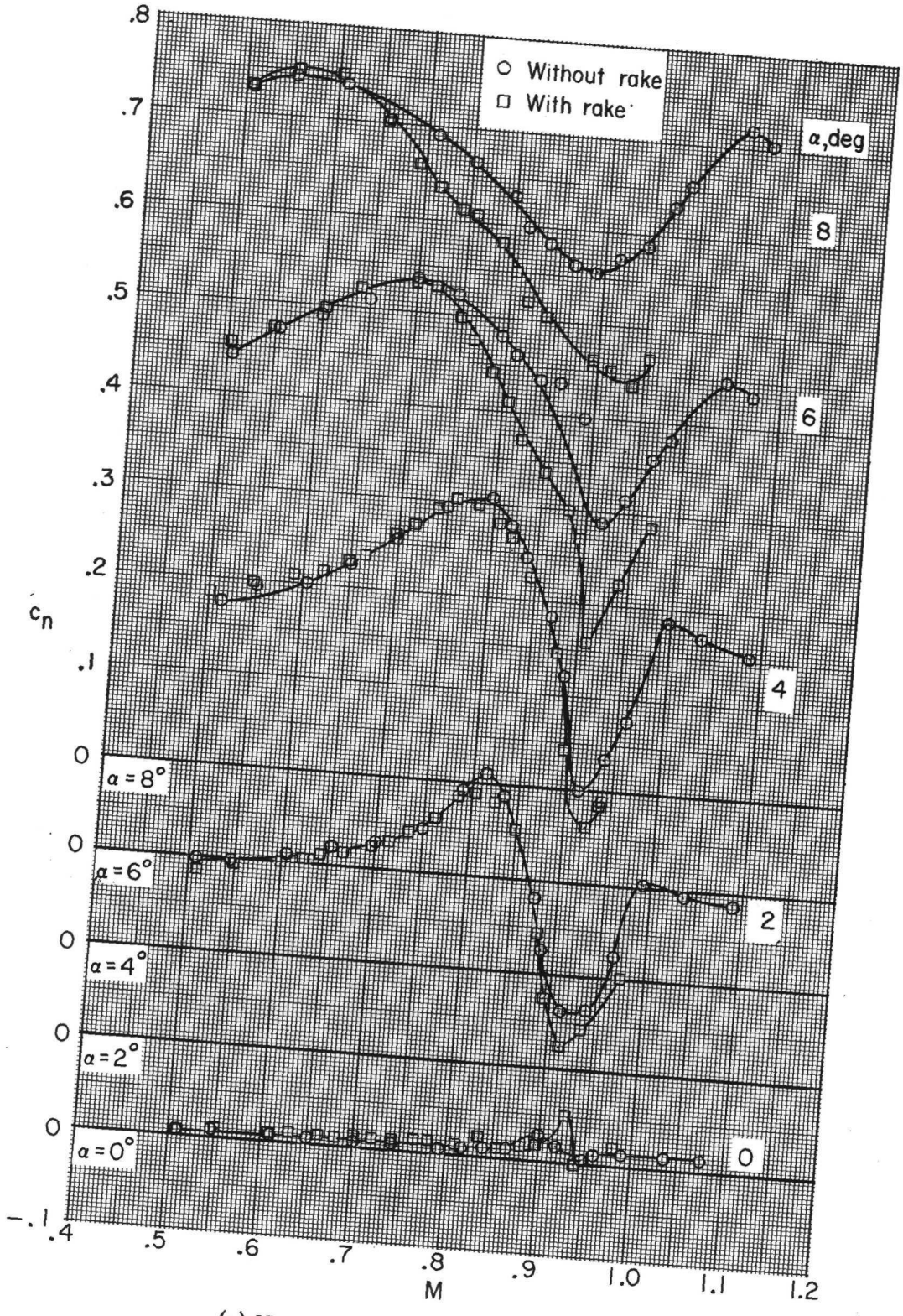


(a) Normal-force coefficient.

Figure 18.- Effects of wake survey rake on aerodynamic characteristics of the NACA 0012 airfoil section.

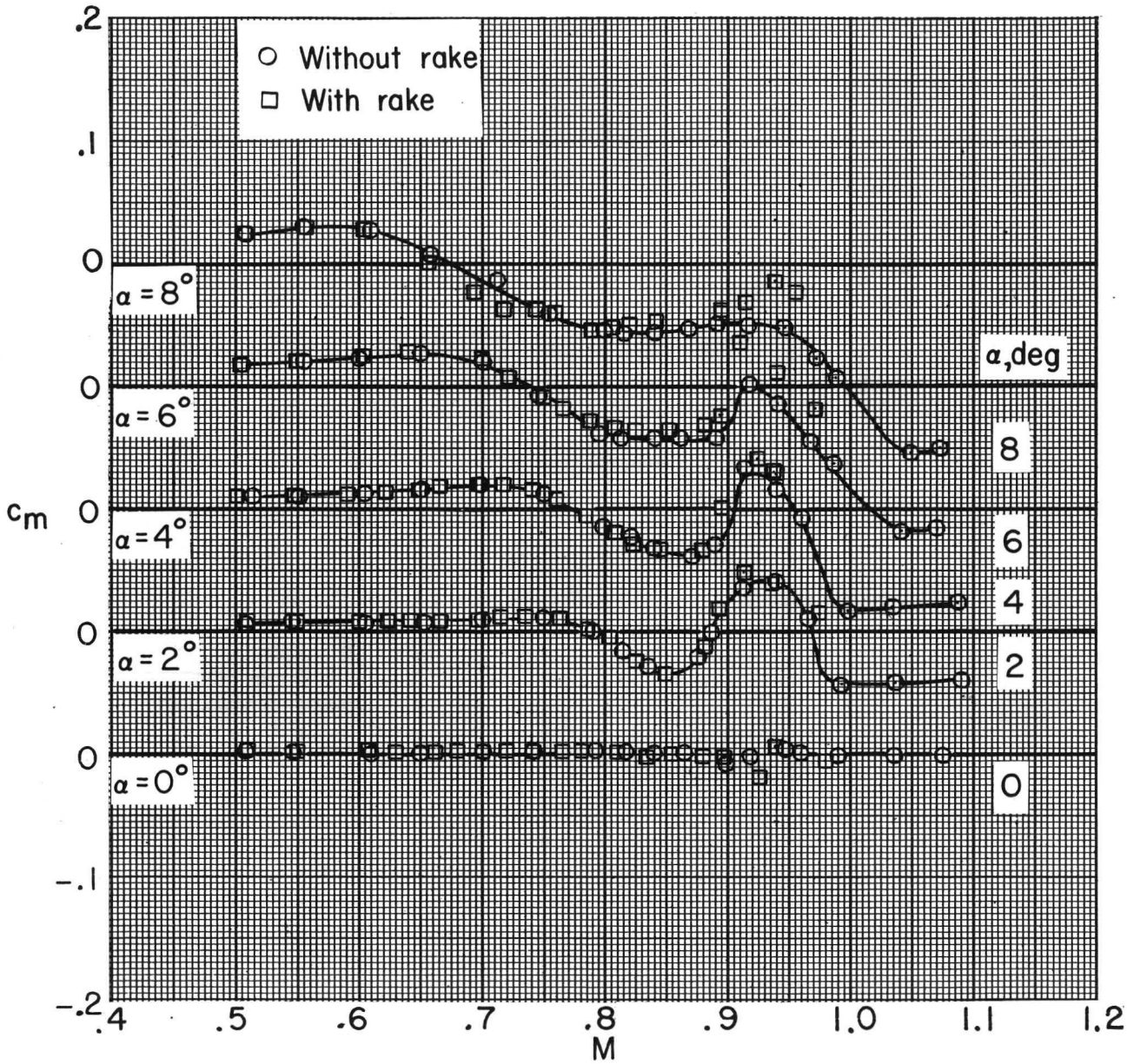


(b) Pitching-moment coefficient.

Figure 18.- Concluded.

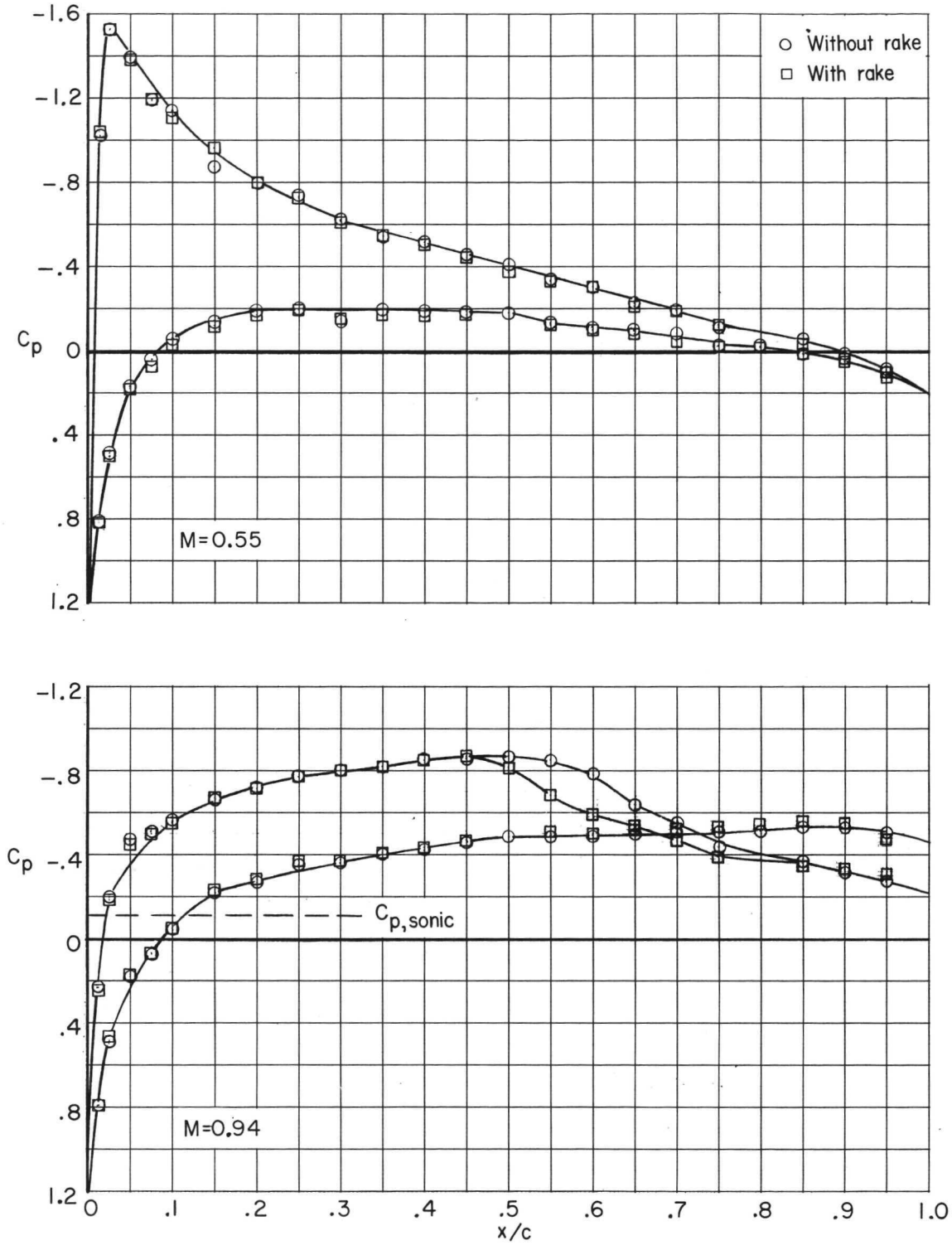


(a) $\alpha = 4^{o}$.

Figure 19.- Effects of wake survey rake on pressure distributions over the NACA 0012 airfoil section.

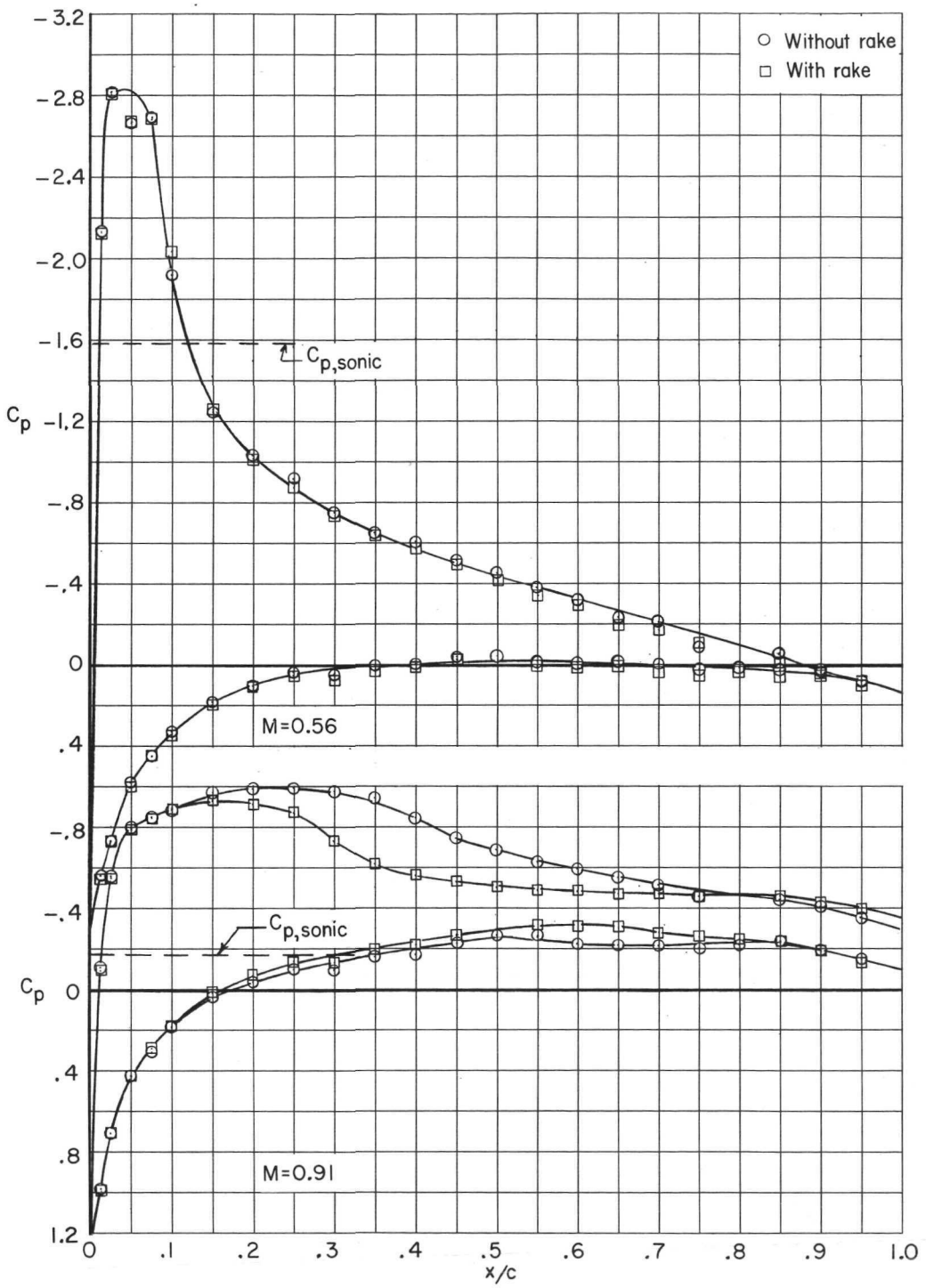


(b) $\alpha = 8^{O}$.

Figure 19.- Concluded.

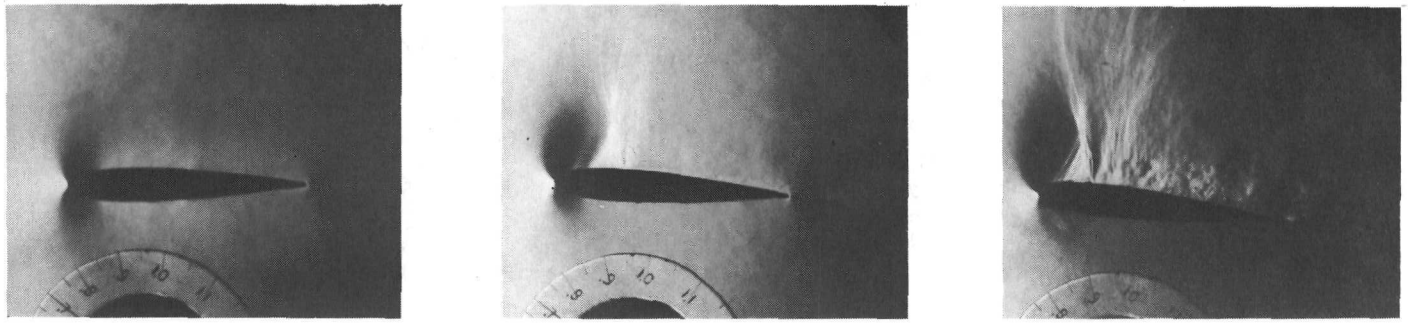

$\alpha = 0^{o}$; M = 0.70 $\alpha = 4^{o}$; M = 0.70 $\alpha = 8^{o}$; M = 0.70

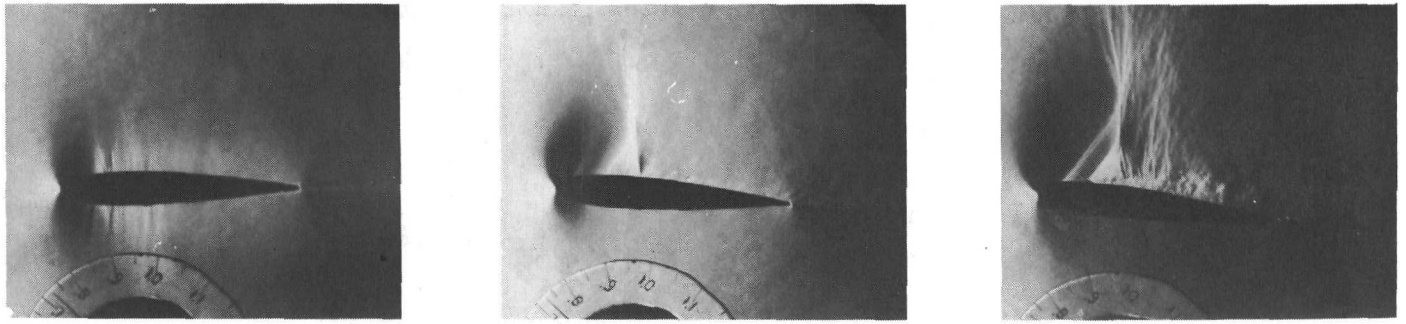

$\alpha = 0^{o}$; M = 0.73 $\alpha = 4^{o}$; M = 0.73 $\alpha = 8^{o}$; M = 0.73

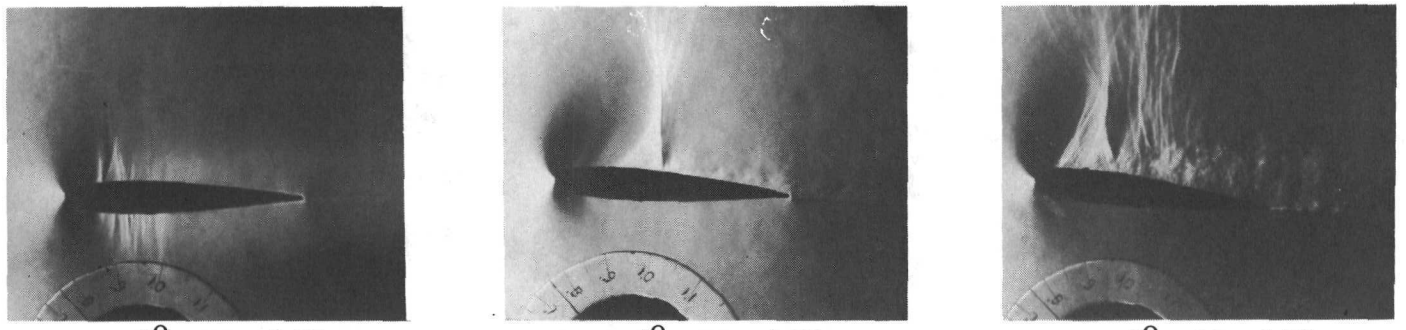

$\alpha = 0^{o}$; M = 0.75 $\alpha = 4^{o}$; M = 0.75 $\alpha = 8^{o}$; M = 0.75

L-73-3004

Figure 20.- Schlieren flow photographs of effects of Mach number and angle of attack on flow pattern of NACA 0012 airfoil section.

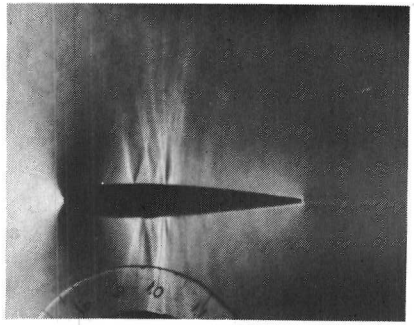

$\alpha = 0^{O}$; M = 0.78

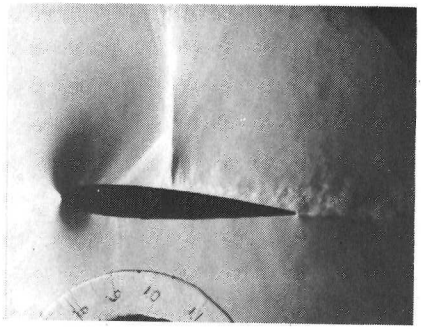

$\alpha = 4^{O}$; M = 0.78

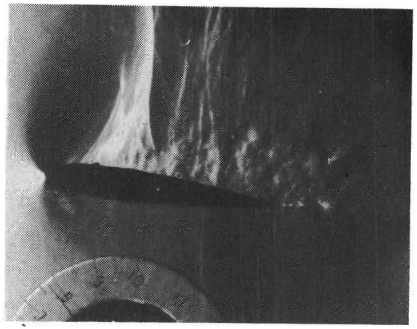

$\alpha = 8^{O}$; M = 0.78

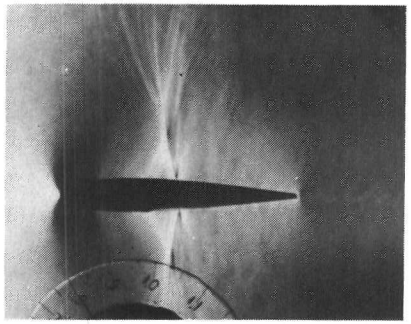

$\alpha = 0^{O}$; M = 0.80

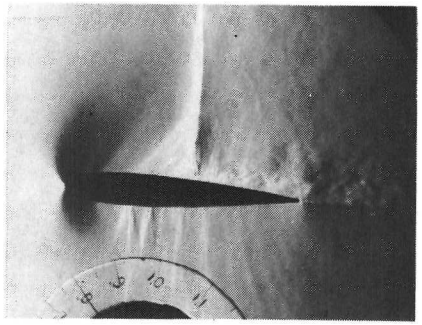

$\alpha = 4^{O}$; M = 0.80

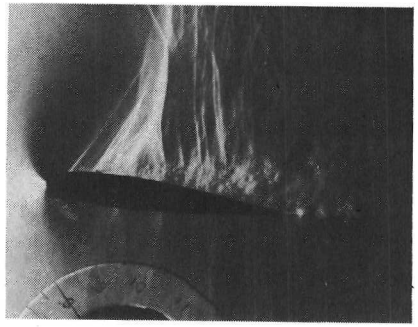

$\alpha = 8^{O}$; M = 0.80

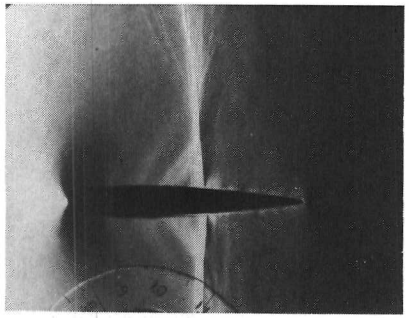

$\alpha = 0^{O}$; M = 0.83

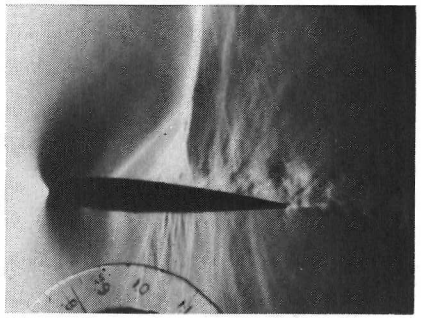

$\alpha = 4^{O}$; M = 0.83

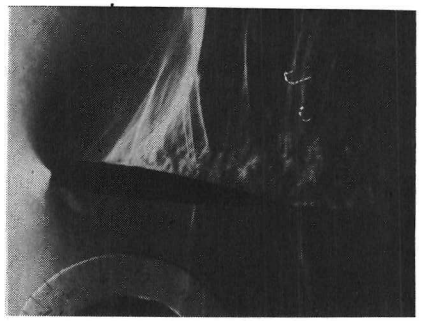

$\alpha = 8^{O}$; M = 0.83

L-73-3005

Figure 20.- Continued.

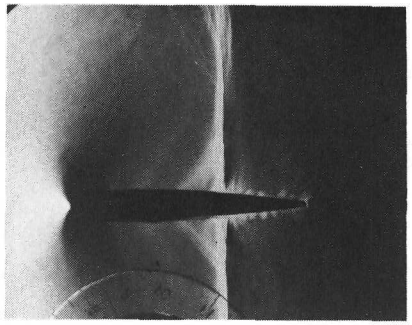

$\alpha = 0^{O}$; M = 0.85

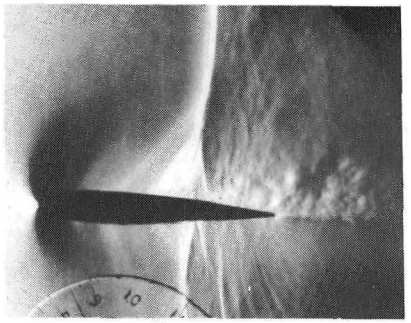

$\alpha = 4^{O}$; M = 0.85

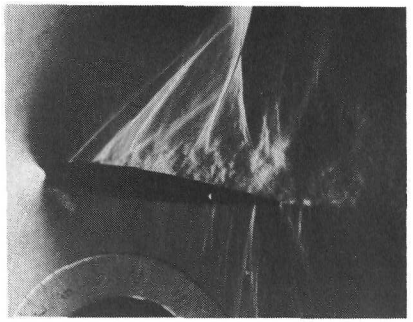

$\alpha = 8^{O}$; M = 0.85

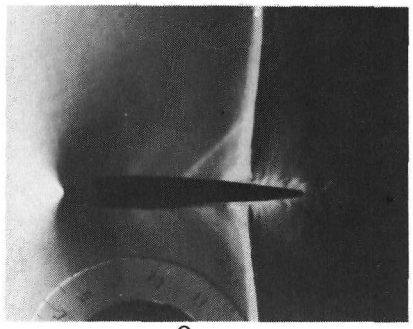

$\alpha = 0^{O}$; M = 0.88

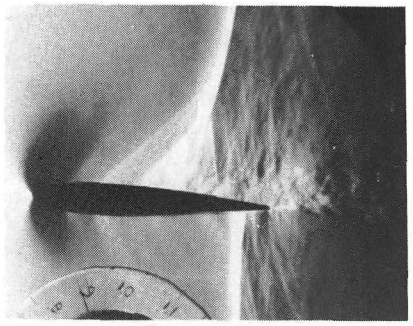

$\alpha = 4^{O}$; M = 0.88

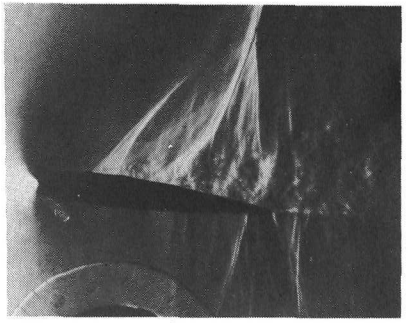

$\alpha = 8^{O}$; M = 0.88

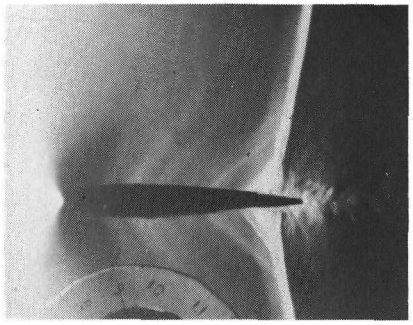

$\alpha = 0^{O}$; M = 0.90

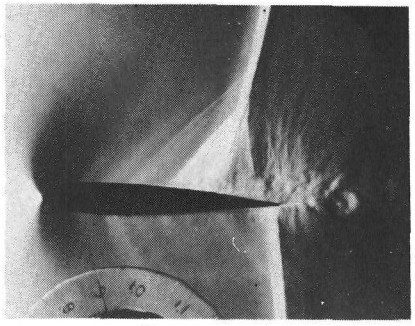

$\alpha = 4^{O}$; M = 0.90

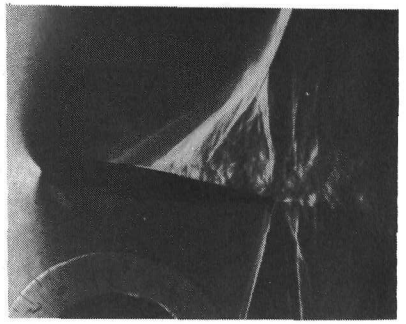

$\alpha = 8^{O}$; M = 0.90

L-73-3006

Figure 20.- Continued.

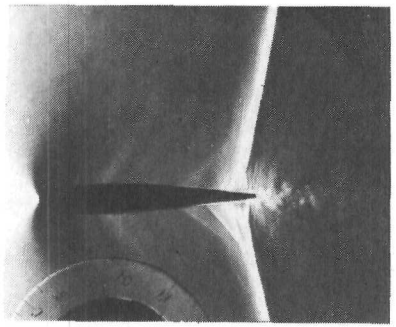

$\alpha = 0^{O}$; M = 0.93

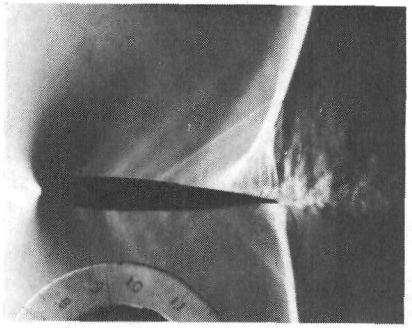

$\alpha = 4^{O}$; M = 0.93

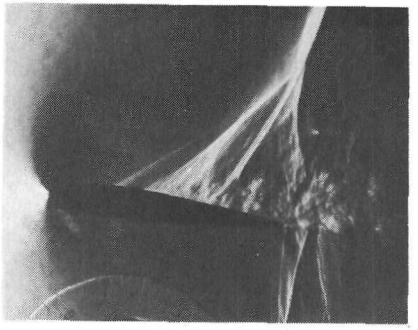

$\alpha = 8^{O}$; M = 0.93

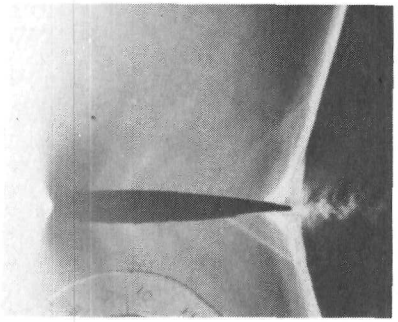

$\alpha = 0^{O}$; M = 0.95

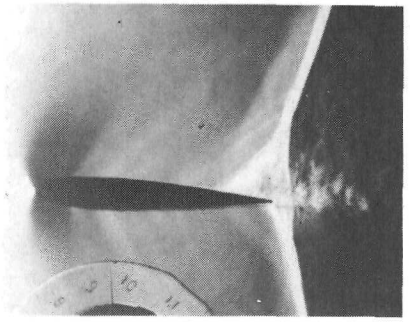

$\alpha = 4^{O}$; M = 0.95

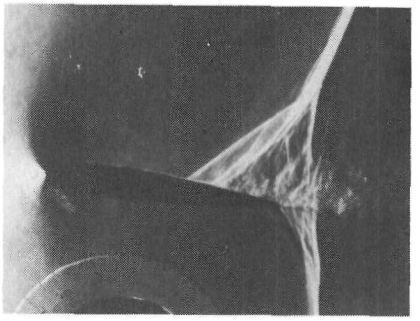

$\alpha = 8^{O}$; M = 0.95

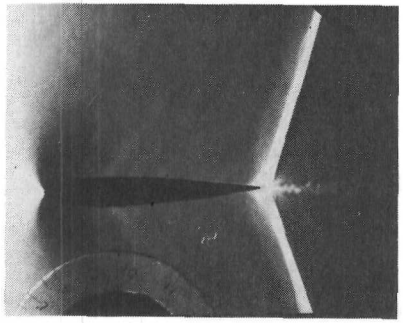

$\alpha = 0^{O}$; M = 0.98

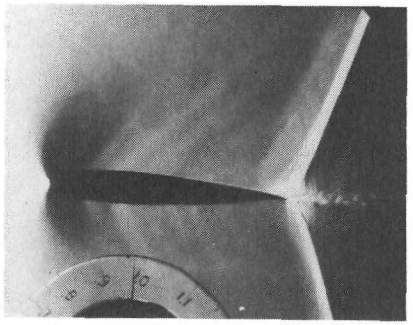

$\alpha = 4^{O}$; M = 0.98

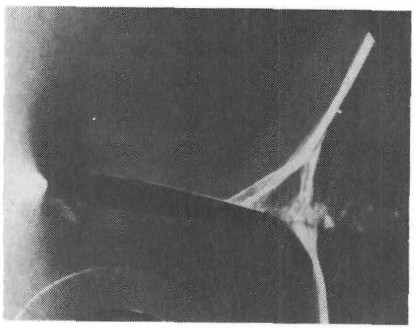

$\alpha = 8^{O}$; M = 0.98

L-73-3007

Figure 20.- Continued.

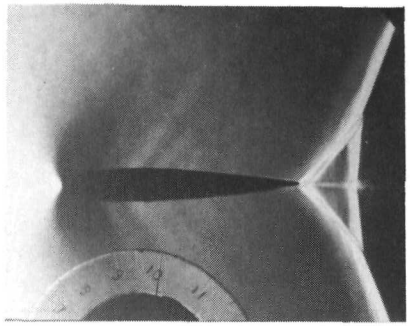

$\alpha = 0^{O}$; M = 1.00

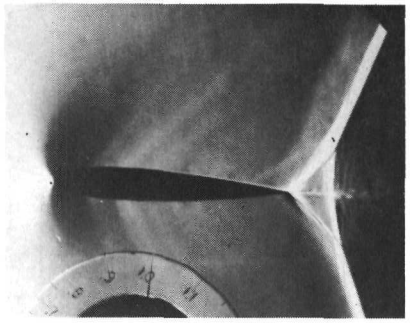

$\alpha = 4^{O}$; M = 1.00

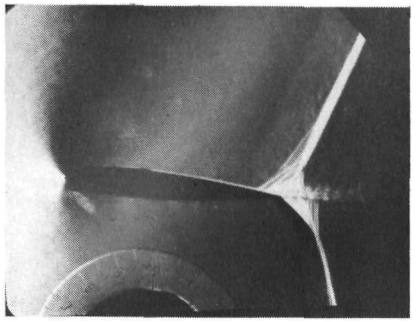

$\alpha = 8^{O}$; M = 1.00

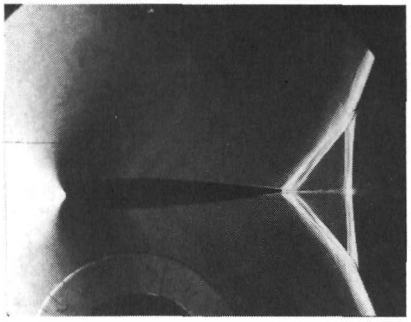

$\alpha = 0^{O}$; M = 1.03

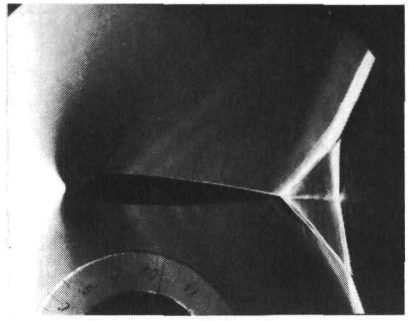

$\alpha = 4^{O}$; M = 1.03

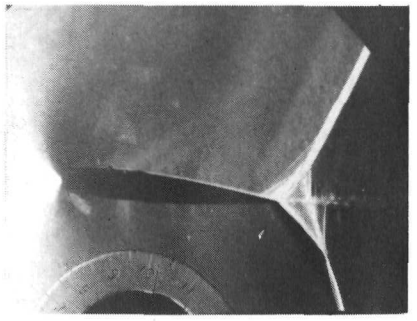

$\alpha = 8^{O}$; M = 1.03

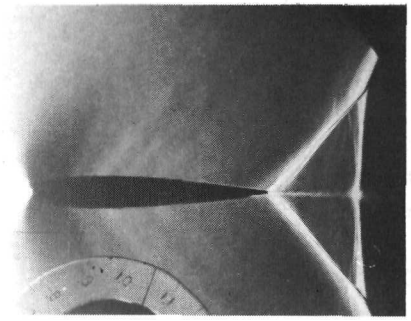

$\alpha = 0^{O}$; M = 1.05

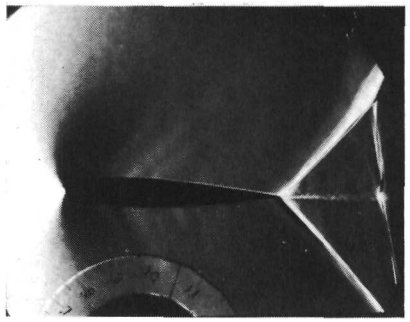

$\alpha = 4^{O}$; M = 1.05

$\alpha = 8^{O}$; M = 1.05

L-73-3008

Figure 20.- Concluded.

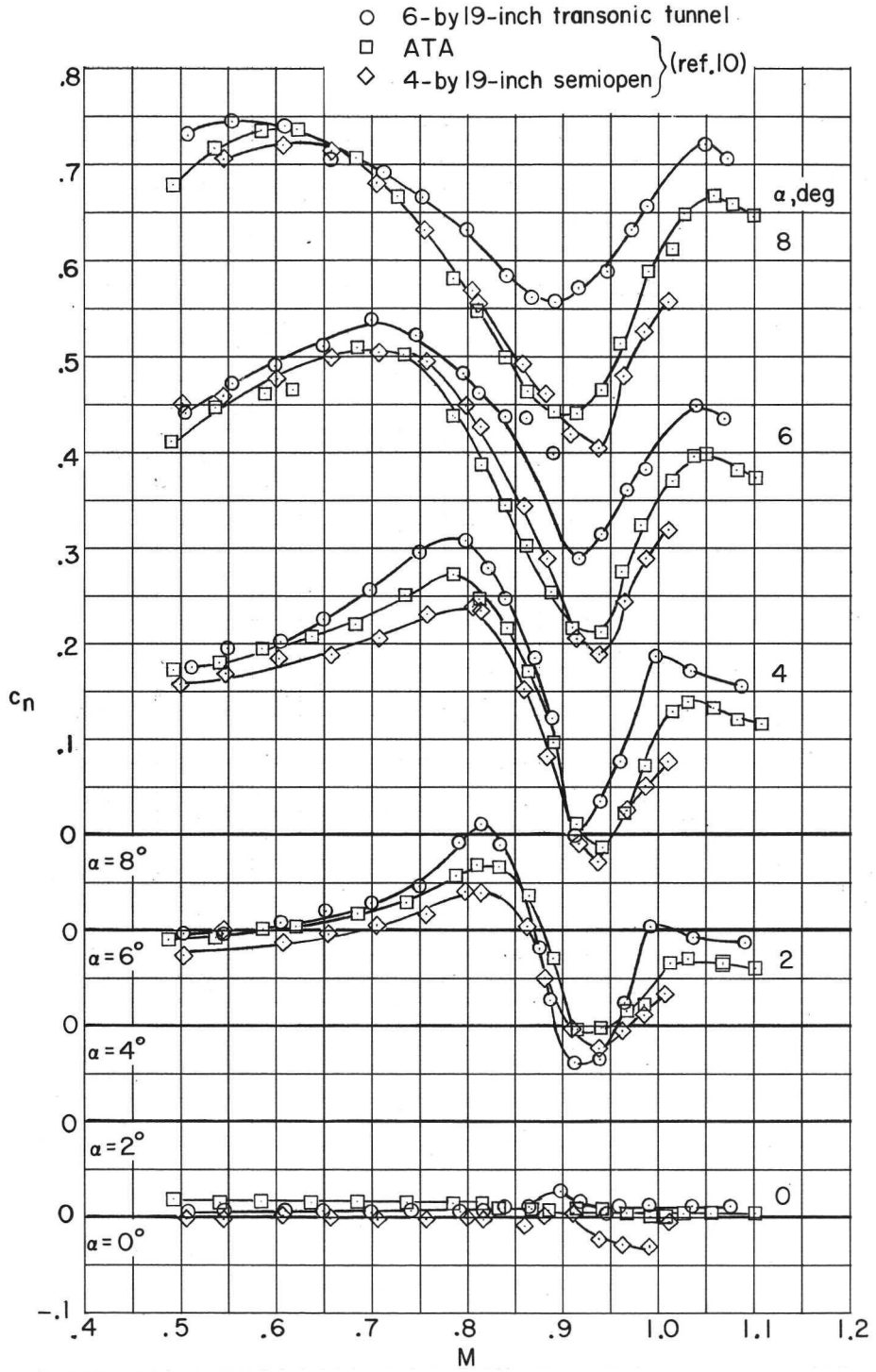


(a) Normal-force coefficient.

Figure 21.- Comparison of aerodynamic characteristics of the NACA 0012 airfoil section obtained in the 6- by 19-inch transonic tunnel with data from other facilities.

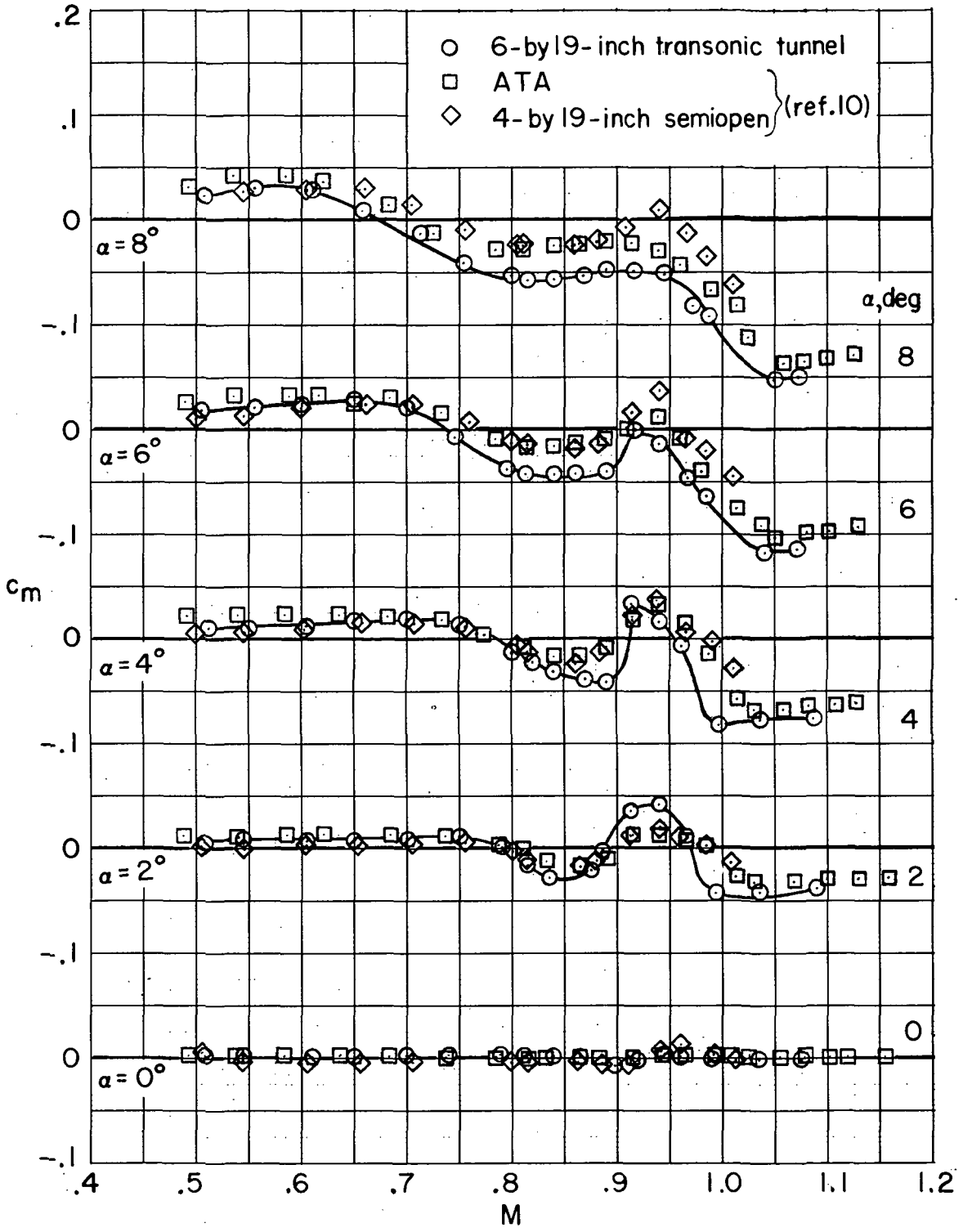


(b) Pitching-moment coefficient.

Figure 21.- Concluded.

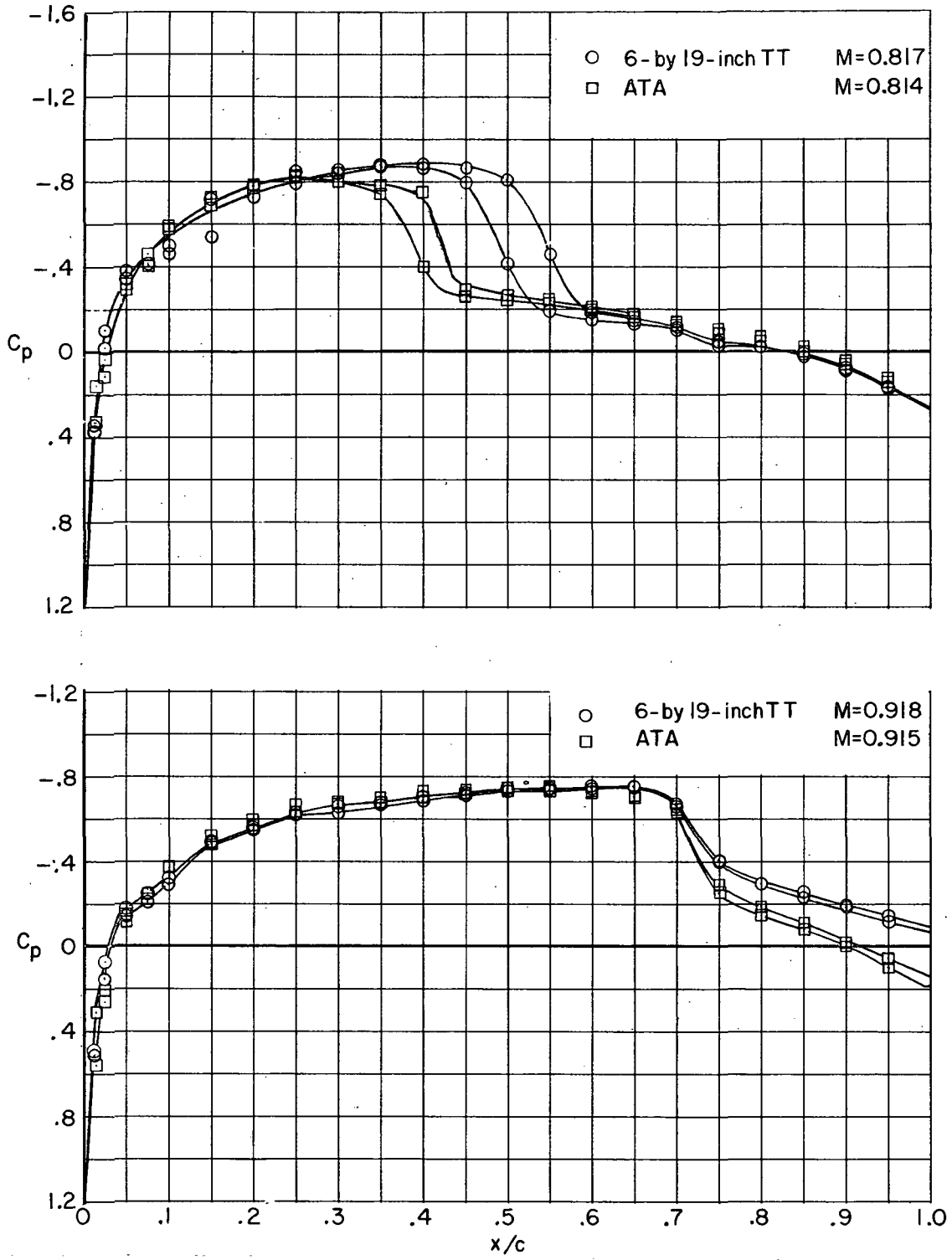


(a) $\alpha = 0^{\circ}$.

Figure 22.- Comparison of surface-pressure distributions over the NACA 0012 airfoil section obtained in the 6- by 19-inch transonic tunnel with unpublished data from the Langley airfoil test apparatus.

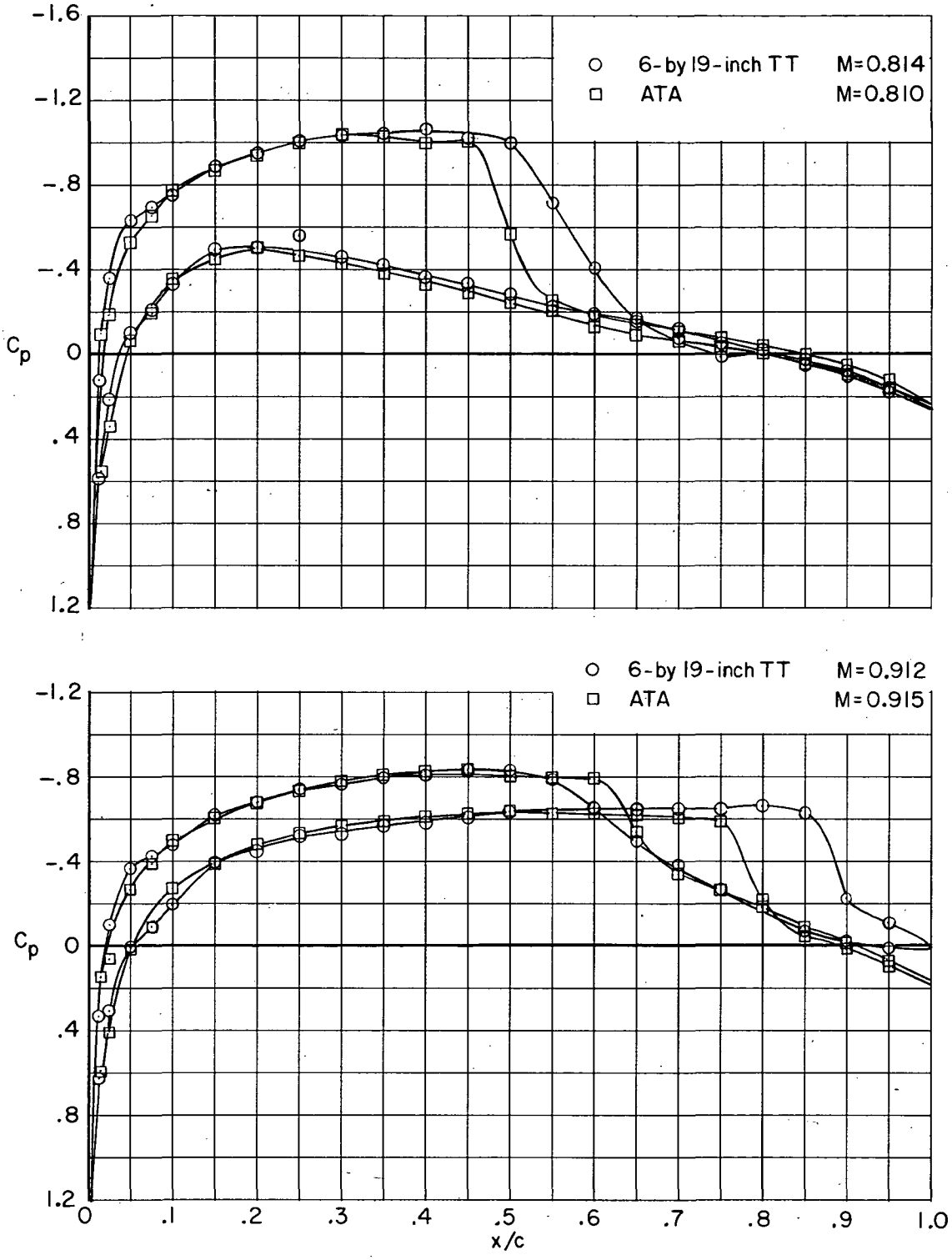


(b) $\alpha = 2^{\circ}$.

Figure 22.- Continued.

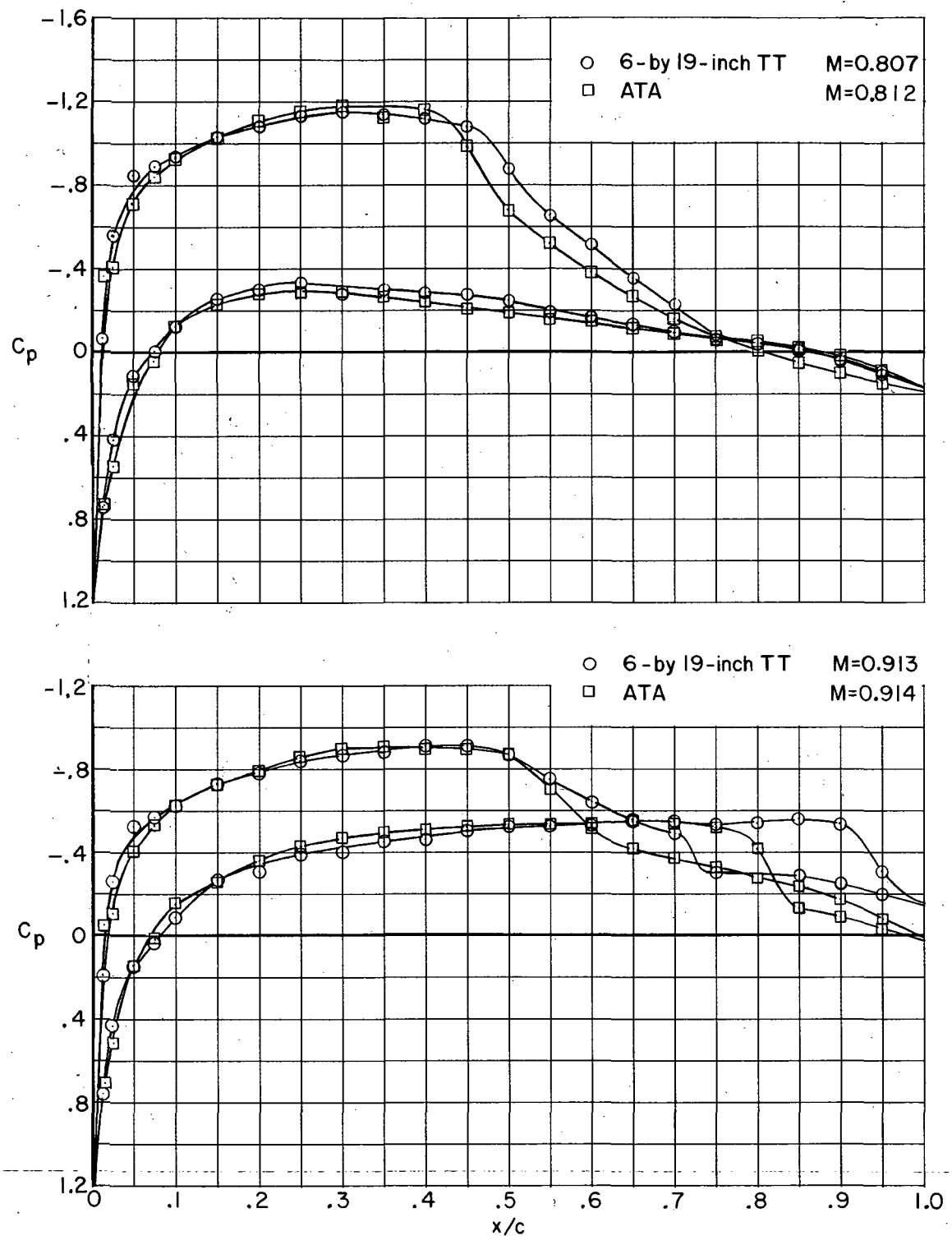


(c) $\alpha = 4^{\circ}$.

Figure 22.- Continued.

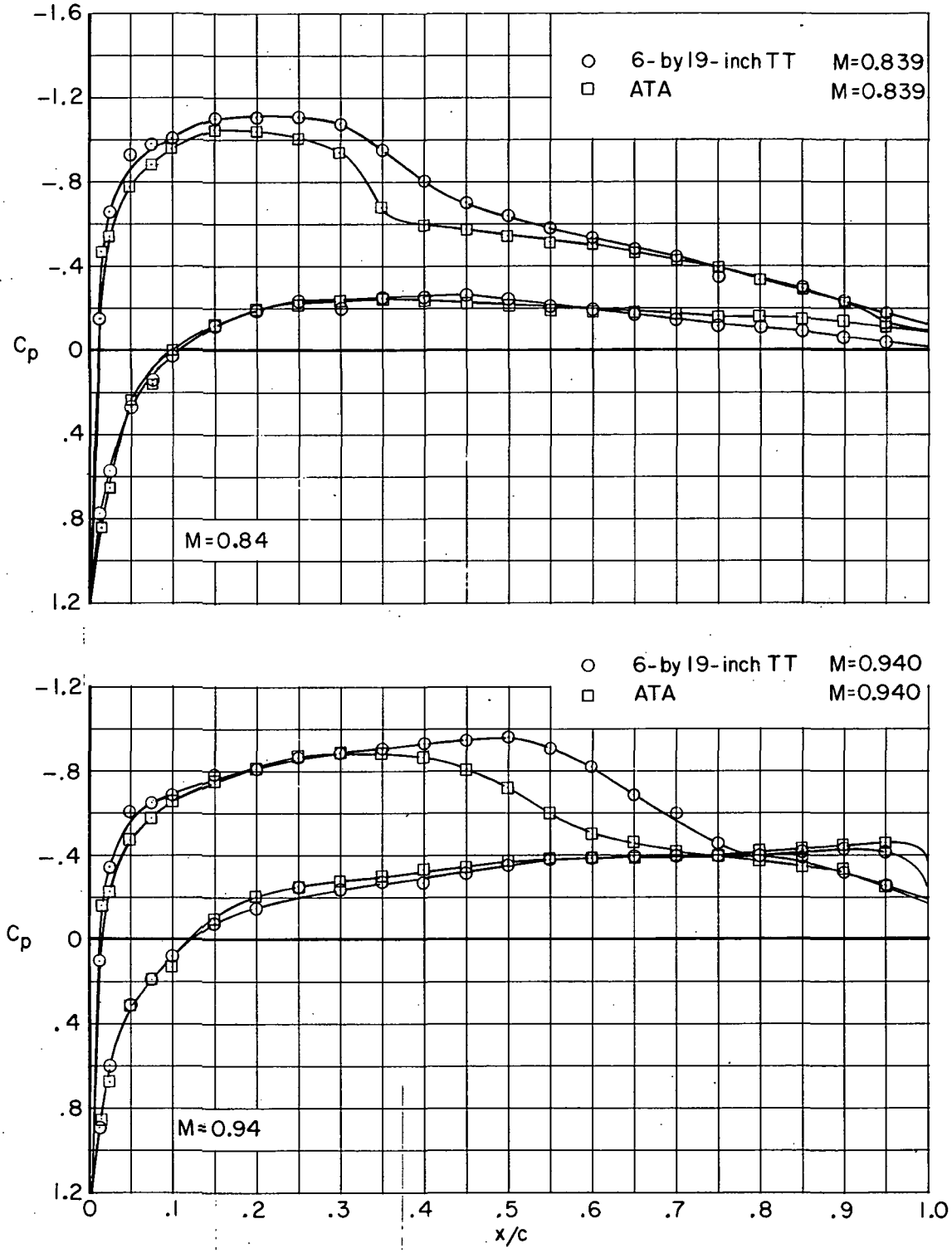


(d) $\alpha = 6^{o}$.

Figure 22.- Continued.

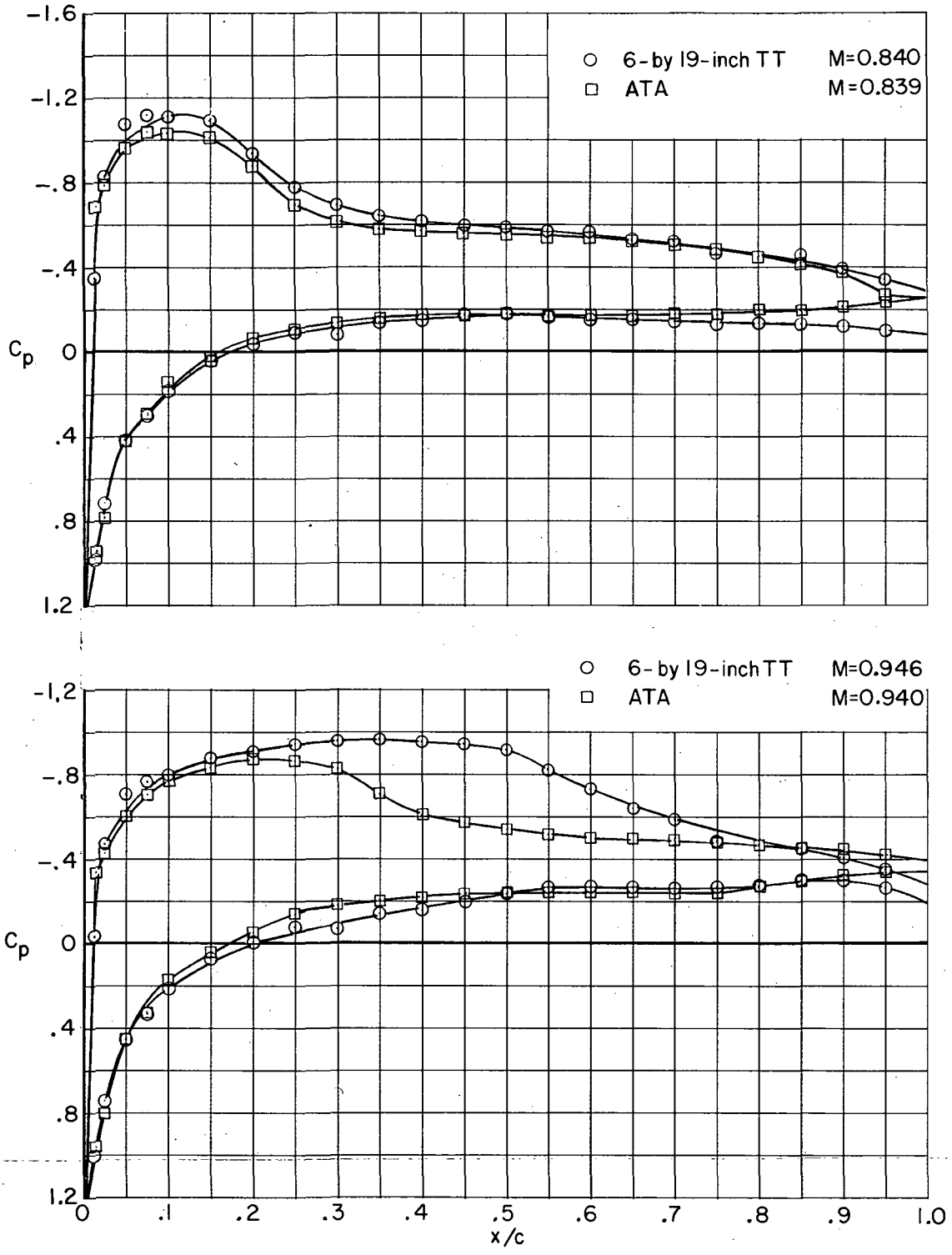


(e) $\alpha = 8^{\circ}$.

Figure 22.- Concluded.

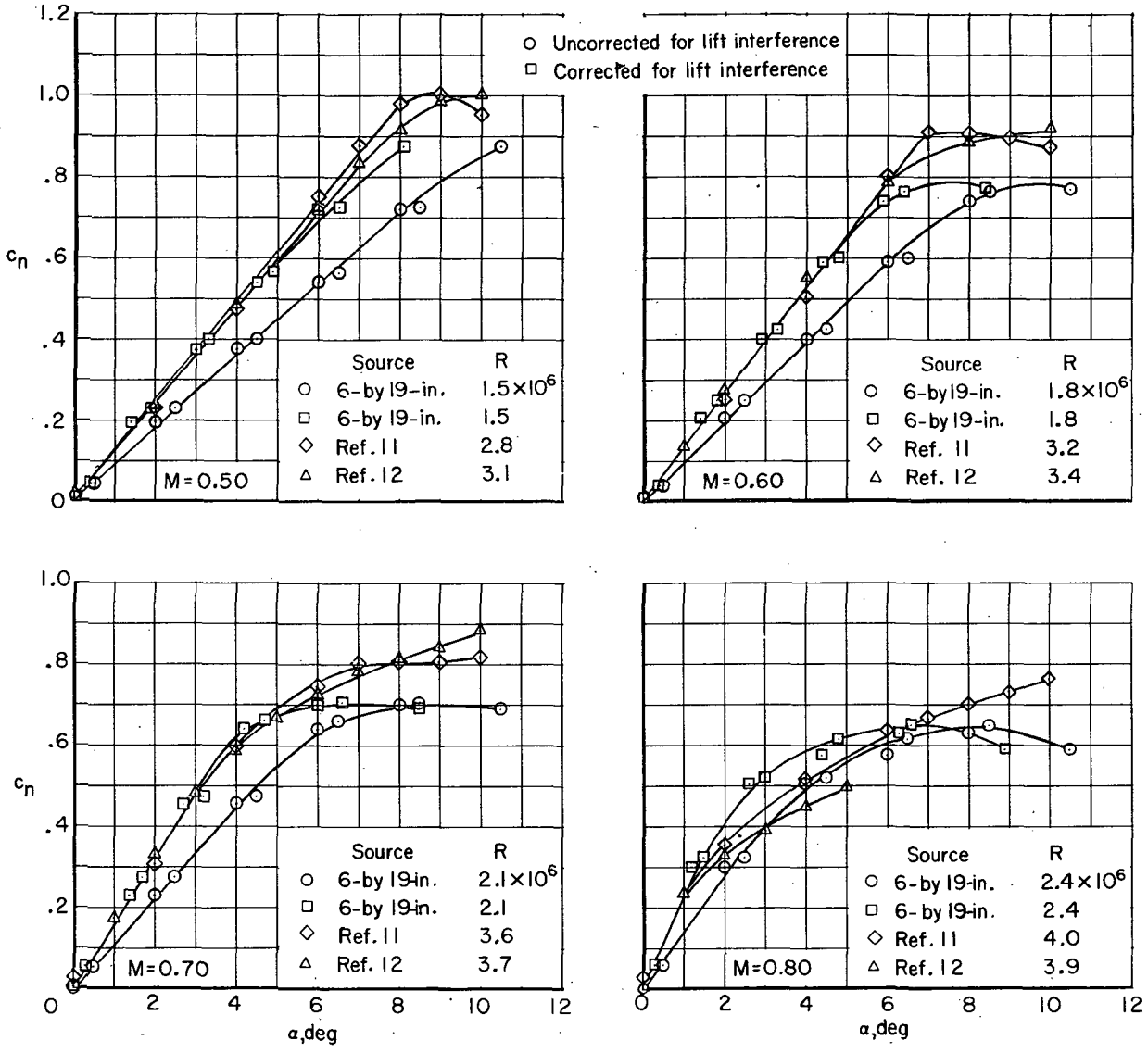


Figure 23.- Comparison of corrected and uncorrected normal-force coefficients for the NACA 0012 airfoil section from the 6- by 19-inch transonic tunnel with data from closed-throat tunnels.

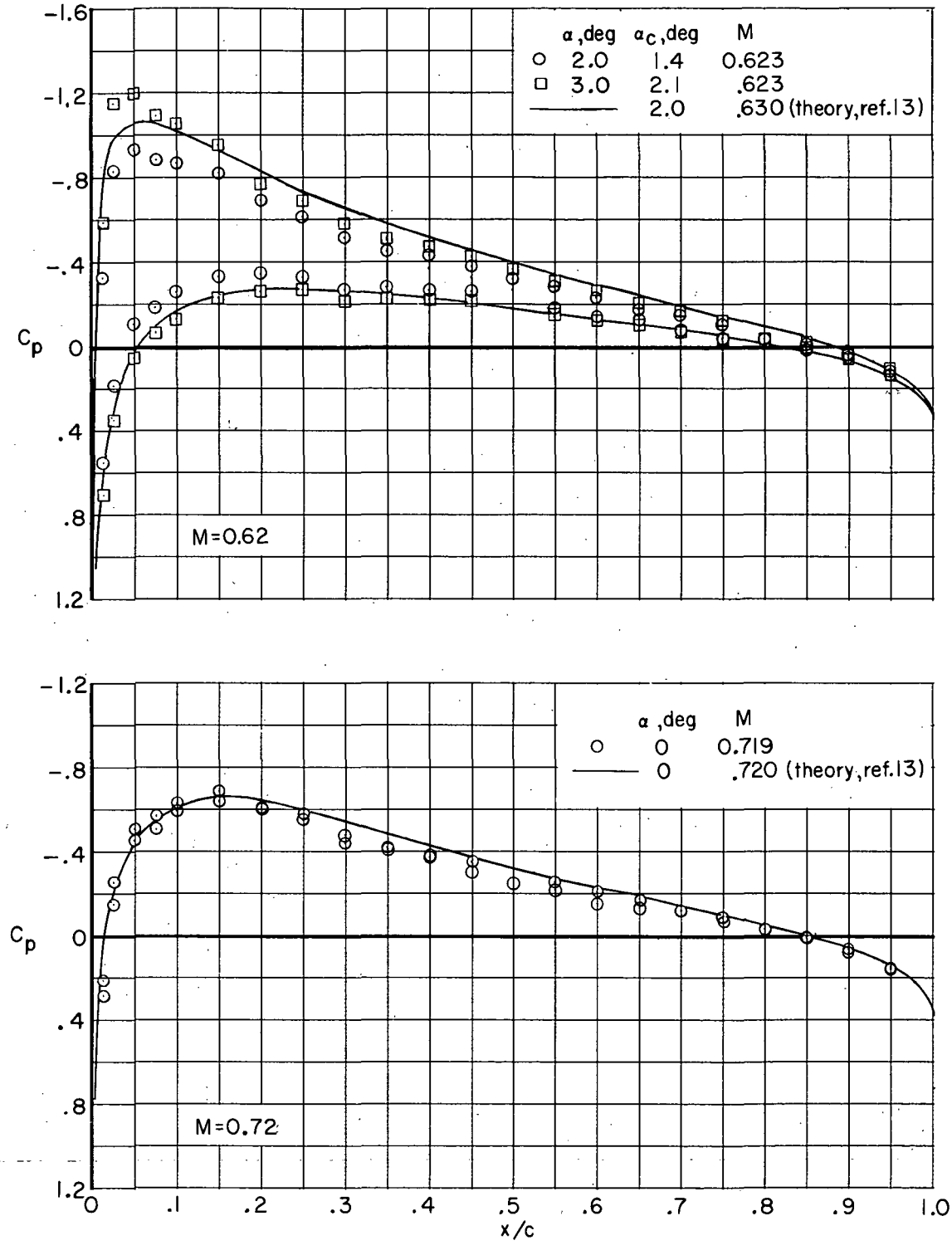


Figure 24.- Comparison of surface-pressure distributions over the NACA 0012 airfoil section from the 6- by 19-inch transonic tunnel with theoretical values from reference 13.

Page Intentionally Left Blank

NATIONAL AERONAUTICS AND SPACE ADMINISTRATION
WASHINGTON, D.C. 20546

OFFICIAL BUSINESS
PENALTY FOR PRIVATE USE $300

SPECIAL FOURTH-CLASS RATE
BOOK

POSTAGE AND FEES PAID
NATIONAL AERONAUTICS AND
SPACE ADMINISTRATION
451

U.S.MAIL

POSTMASTER: If Undeliverable (Section 158 Postal Manual) Do Not Return

*"The aeronautical and space activities of the United States shall be conducted so as to contribute . . . to the expansion of human knowledge of phenomena in the atmosphere and space. The Administration shall provide for the widest practicable and appropriate dissemination of information concerning its activities and the results thereof."*

—NATIONAL AERONAUTICS AND SPACE ACT OF 1958

# NASA SCIENTIFIC AND TECHNICAL PUBLICATIONS

TECHNICAL REPORTS: Scientific and technical information considered important, complete, and a lasting contribution to existing knowledge.

TECHNICAL NOTES: Information less broad in scope but nevertheless of importance as a contribution to existing knowledge.

TECHNICAL MEMORANDUMS: Information receiving limited distribution because of preliminary data, security classification, or other reasons. Also includes conference proceedings with either limited or unlimited distribution.

CONTRACTOR REPORTS: Scientific and technical information generated under a NASA contract or grant and considered an important contribution to existing knowledge.

TECHNICAL TRANSLATIONS: Information published in a foreign language considered to merit NASA distribution in English.

SPECIAL PUBLICATIONS: Information derived from or of value to NASA activities. Publications include final reports of major projects, monographs, data compilations, handbooks, sourcebooks, and special bibliographies.

TECHNOLOGY UTILIZATION PUBLICATIONS: Information on technology used by NASA that may be of particular interest in commercial and other non-aerospace applications. Publications include Tech Briefs, Technology Utilization Reports and Technology Surveys.

***Details on the availability of these publications may be obtained from:***

**SCIENTIFIC AND TECHNICAL INFORMATION OFFICE**

**NATIONAL AERONAUTICS AND SPACE ADMINISTRATION**

**Washington, D.C. 20546**